



中国科学院高能物理研究所
Institute of High Energy Physics
Chinese Academy of Sciences



Measurement of $B^0_{(s)} \rightarrow \pi^0\pi^0$ at CEPC

Yuexin Wang, Manqi Ruan

CEPC Day, September 22, 2021

Outline

- 1. Motivation**
- 2. Separation of B^0 and B^0_s**
- 3. Event selection**
- 4. Dependence on b-tagging performance**
- 5. Dependence on B mass resolution**
- 6. Summary**

Motivation

From **physics** aspect

- $B^0 \rightarrow \pi^0 \pi^0$ combined with $B^0 \rightarrow \pi^+ \pi^-$ and $B^+ \rightarrow \pi^+ \pi^0$, golden channels to determine the CKM angle: α (Φ_2)
- “ $B \rightarrow \pi\pi$ puzzle”, the measured branching ratio of the $B^0 \rightarrow \pi^0 \pi^0$ is significantly larger than the theoretical predictions.
- $B^0_s \rightarrow \pi^0 \pi^0$, a pure annihilation process, BR $\sim 10^{-7}$, has not been observed.
- Tera-Z at CEPC with 10^{11} B^0 and 10^{10} B^0_s , at least 1-2 orders larger than Belle-II

Modes	DATA [1]	SCET [2]	QCDF	pQCD
$B^+ \rightarrow \pi^+ \pi^0$	5.5 ± 0.4	5.20 ± 2.71	$6.00^{+3.76}_{-3.07}$	$4.27^{+1.85}_{-1.47}$
$B^0 \rightarrow \pi^+ \pi^-$	5.12 ± 0.19	5.40 ± 1.95	$8.90^{+5.55}_{-4.71}$	$7.67^{+3.27}_{-2.67}$
$B^0 \rightarrow \pi^0 \pi^0$	1.59 ± 0.26	0.84 ± 0.46	$0.30^{+0.46}_{-0.26}$	$0.24^{+0.09}_{-0.07}$
$B^0_s \rightarrow \pi^+ \pi^-$	0.7 ± 0.1	-	$0.26^{+0.10}_{-0.09}$	$0.52^{+0.21}_{-0.18}$
$B^0_s \rightarrow \pi^0 \pi^0$	< 210	-	$0.13^{+0.05}_{-0.05}$	$0.21^{+0.10}_{-0.09}$

Table 1: Experimental measurements and theoretical predictions of the branching ratios (in unit of 10^{-6}) of $B \rightarrow \pi\pi$ system. The soft collinear effective theory (SCET), QCD factorization (QCDF), and perturbative QCD (pQCD) are three common theoretical techniques to deal with the hadronic B-meson decays.

From **detector** aspect

Clear dependence on the detector performance

- b-tagging
- ECAL performance

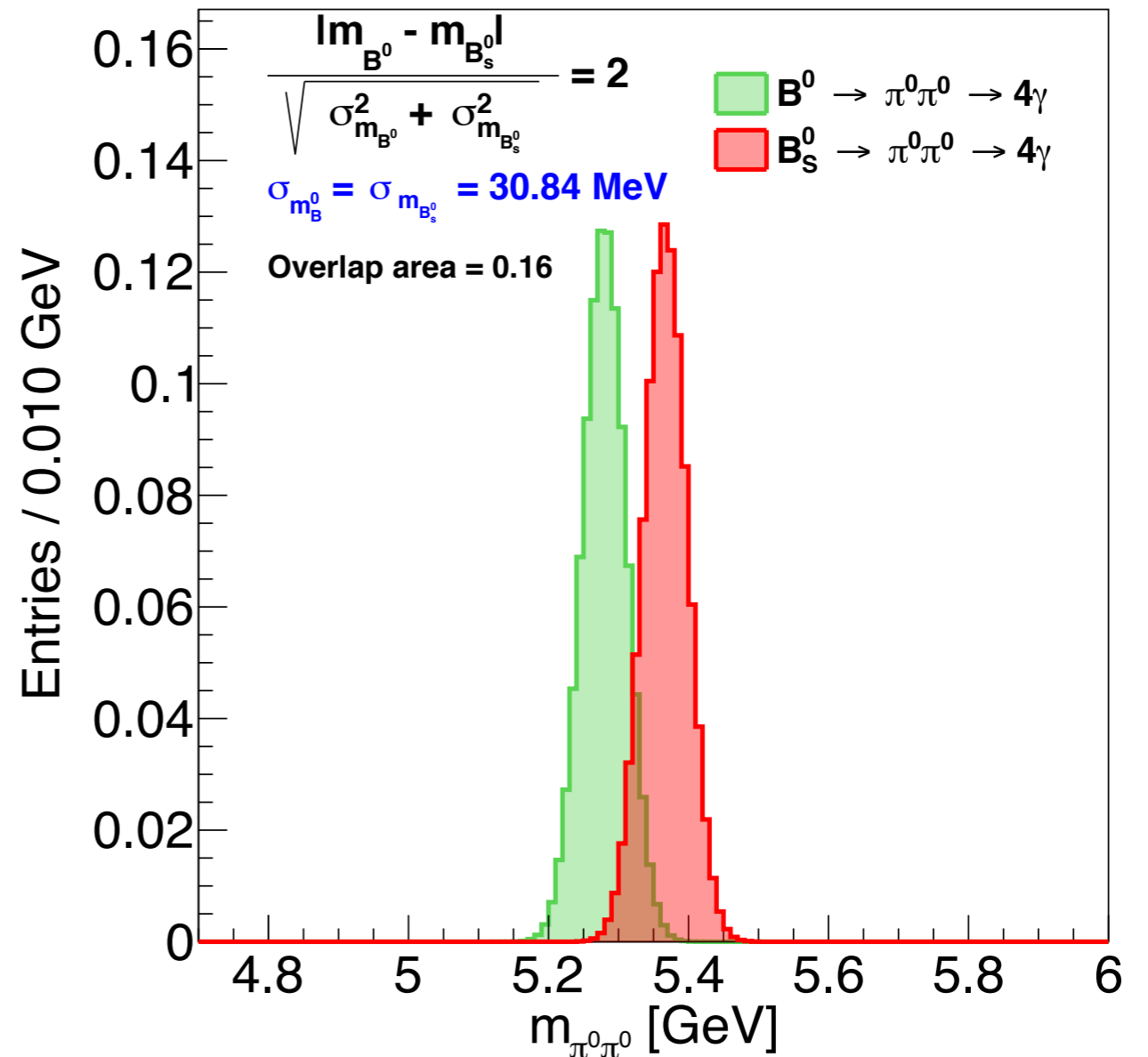
A Fast Simulation Analysis

Separation of B^0 and B_s^0

B meson mass

m_{B^0}	$5279.65 \pm 0.12 \text{ MeV}$
$m_{B_s^0}$	$5366.88 \pm 0.14 \text{ MeV}$
$m_{B_s^0} - m_{B^0}$	$87.38 \pm 0.16 \text{ MeV}$

$$\text{separation power} = \frac{|\bar{m}_{B^0} - \bar{m}_{B_s^0}|}{\sqrt{\sigma_{m_{B^0}}^2 + \sigma_{m_{B_s^0}}^2}}$$

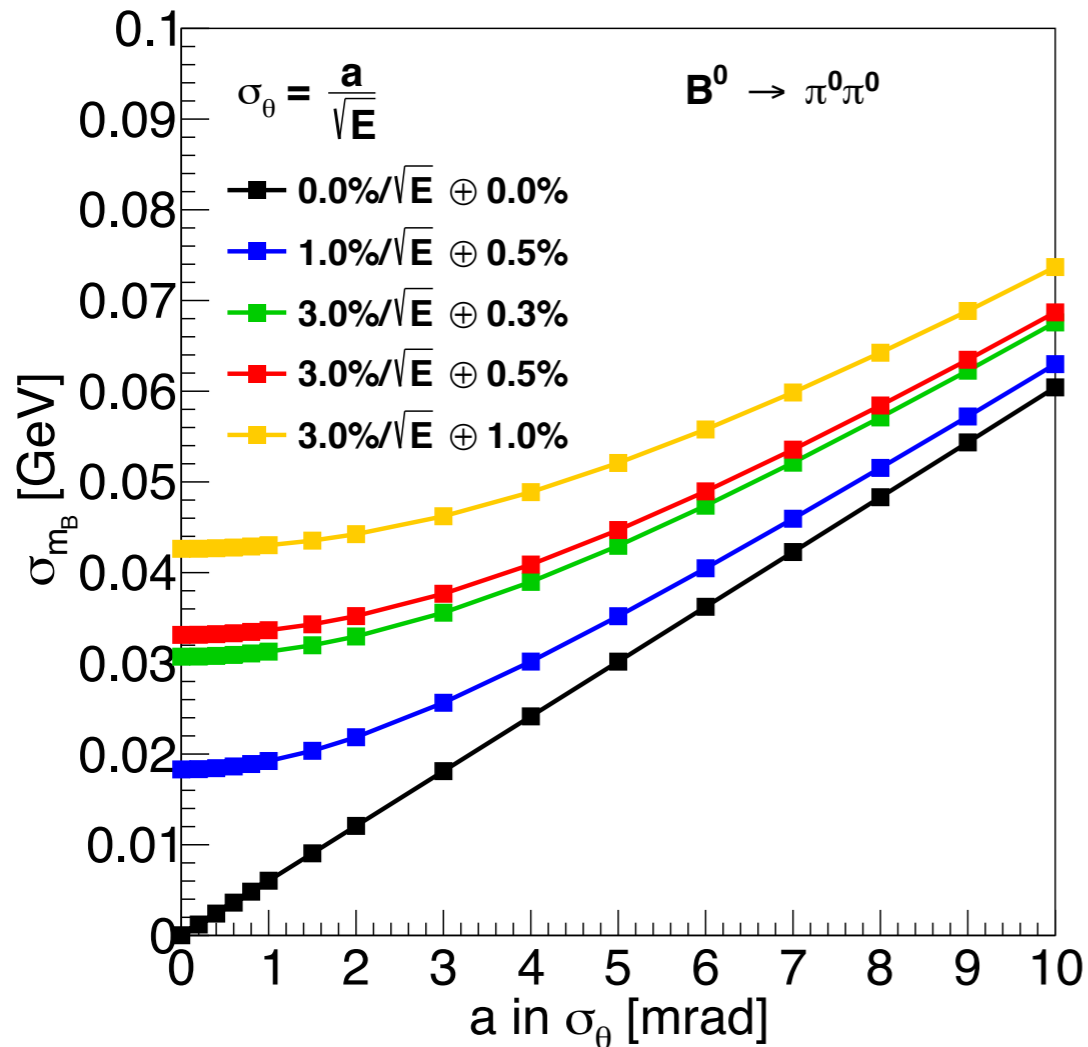


2σ separation requires B mass resolution σ_{m_B} better than 30 MeV.

Dependence of B mass resolution on detector performance

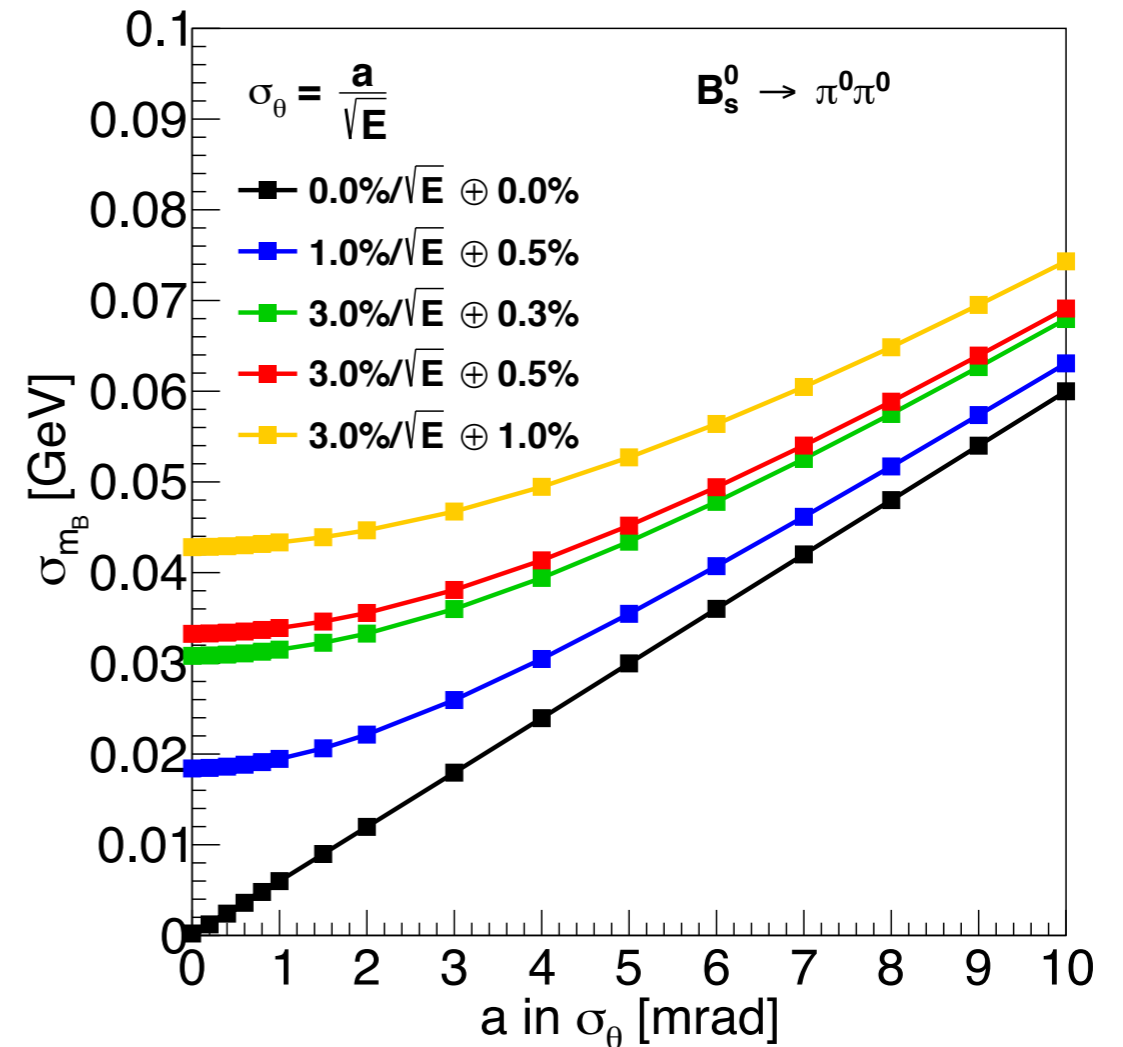
ECAL energy resolution

$$\frac{\sigma_E}{E} = \frac{A}{\sqrt{E}} \oplus C$$



Photon angular resolution

$$\sigma_\theta = \frac{a}{\sqrt{E}}, \quad \sigma_\phi = \frac{\sigma_\theta}{\sin\theta}$$

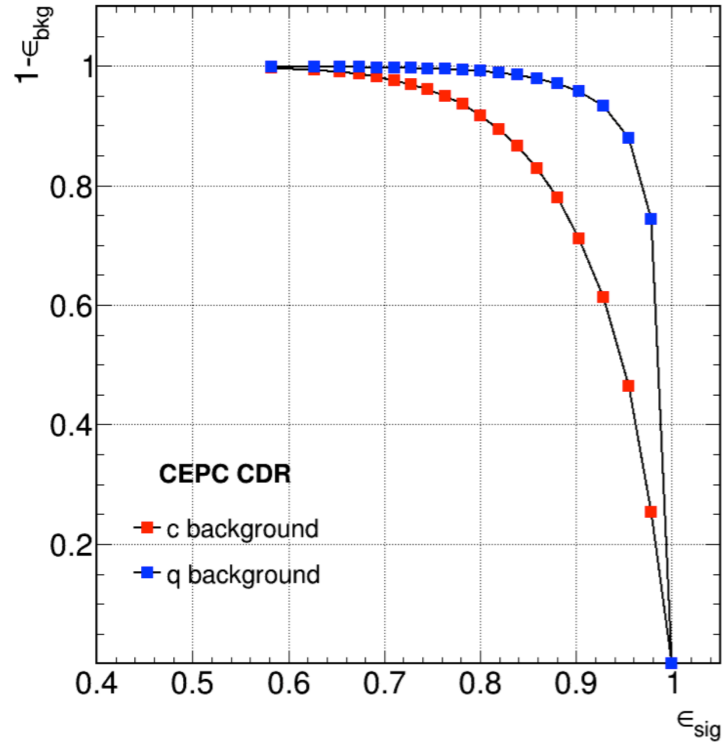


- CEPC baseline single photon angular resolution $\sim 1\text{mrad}/\sqrt{E}$
- ECAL energy resolution dominates the contribution when $\sigma_\theta < 1\text{mrad}/\sqrt{E}$
- The following analysis only takes ECAL energy resolution into account
- $\sigma_{m_B} \sim 30\text{ MeV}$ requires ECAL energy resolution $\sim 3\%/\sqrt{E} \oplus 0.3\%$

Event Selection

CEPC baseline b-tagging

80% efficiency and 90% purity



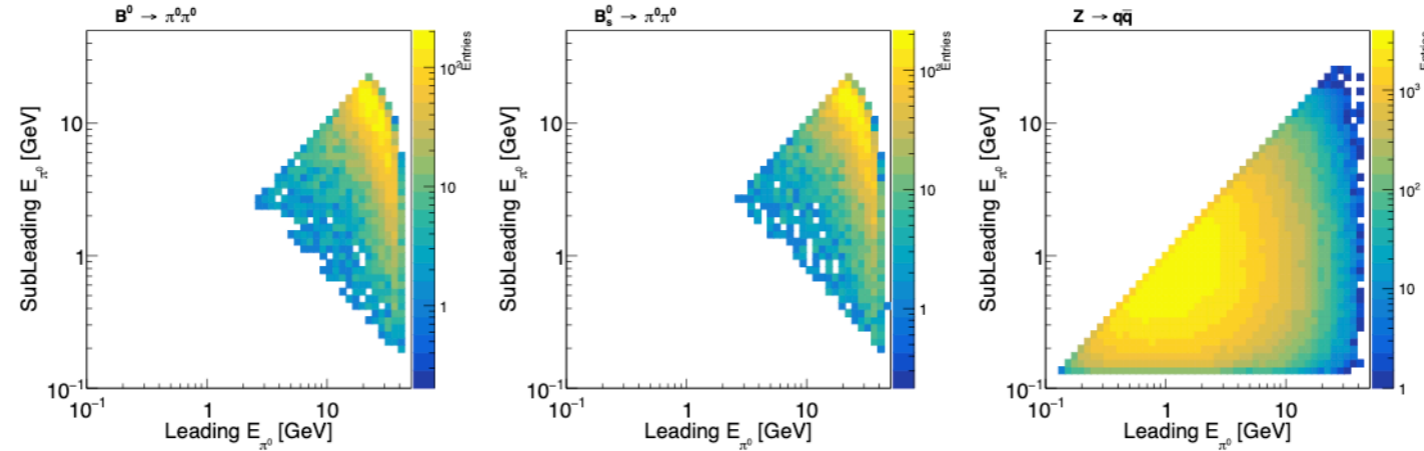
Numerical values used to estimate the signal statistics at Tera-Z.

$f(b \rightarrow B^0)$	0.407 ± 0.007
$f(b \rightarrow B_s^0)$	0.101 ± 0.008
$Br(B^0 \rightarrow \pi^0 \pi^0)$	1.59×10^{-6}
$Br(B_s^0 \rightarrow \pi^0 \pi^0)$	3×10^{-7} SM prediction
$Br(\pi^0 \rightarrow \gamma\gamma)$	98.823%

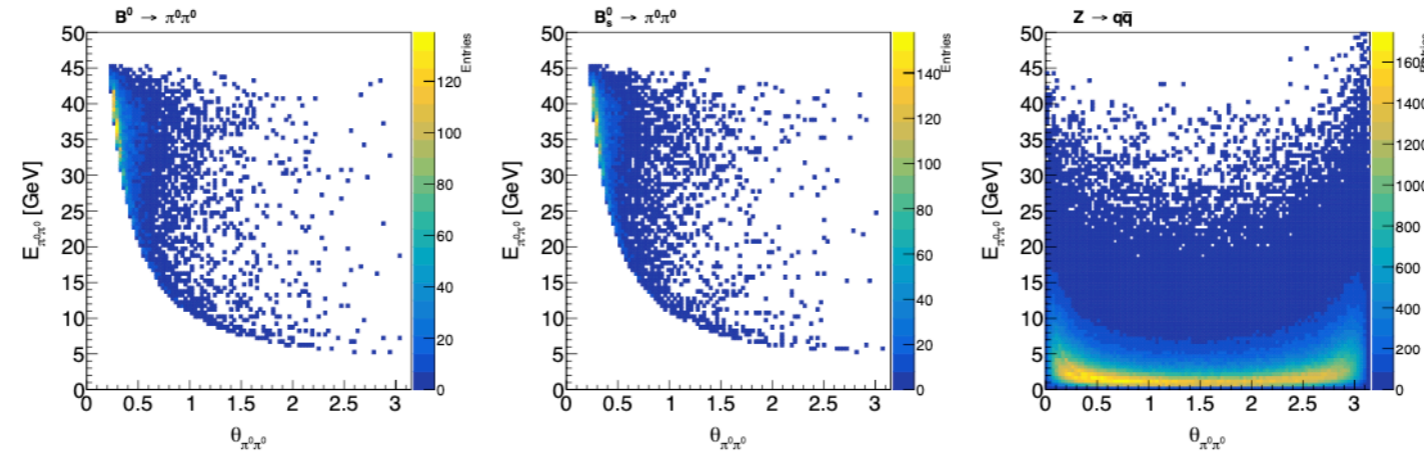
Cut chain table at 3%/√E ⊕ 0.3% & CEPC baseline b-tagging

Cut chain	$B^0 \rightarrow \pi^0 \pi^0$	$B_s^0 \rightarrow \pi^0 \pi^0$	$q\bar{q}$	$u\bar{u} + d\bar{d} + s\bar{s}$	$c\bar{c}$	$b\bar{b}$	$\sqrt{S} + B/S$
Total generated	191113	8948	7e11 (100.00%)	4.285e11 (61.21%)	1.203e11 (17.19%)	1.512e11 (21.60%)	
b-tagging ($\epsilon_{b,c,uds \rightarrow b} = 80\%, 8.26\%, 0.85\%$)	152890	7158	1.34539e11 (100.00%)	3.64225e9 (2.70%)	9.93678e9 (7.38%)	1.2096e11 (89.92%)	
$\pi^0 \rightarrow \gamma\gamma$	147932	6959	134272699126	3605151069	9908563142	120758984915	
Lower $E_{\pi^0} > 6$ GeV	92172	4396	15490570779	843830534	1598643569	13048096676	
Higher $E_{\pi^0} > 14$ GeV	87057	4148	2534286670	307734259	314762436	1911789975	
$E_{\pi^0 \pi^0} > 22$ GeV	86807	4133	2233308564	289771547	281656846	1661880170	
$\theta_{\pi^0 \pi^0} < 23^\circ$	77626	3644	825367542	119076559	102055313	604235671	
$m_{\pi^0 \pi^0} \in (5.2188, 5.3405)$ GeV ($2.0 \sigma_{m_{B^0}} = 2.0 \times 0.0304$ GeV)	75374	717	17896	5640	1656	10600	0.4067% ± 0.0106%
$m_{\pi^0 \pi^0} \in (5.3421, 5.3917)$ GeV ($0.8 \sigma_{m_{B_s^0}} = 0.8 \times 0.0310$ GeV)	3769	2394	5477	2400	507	2570	4.5070% ± 0.5563%

Event Selection



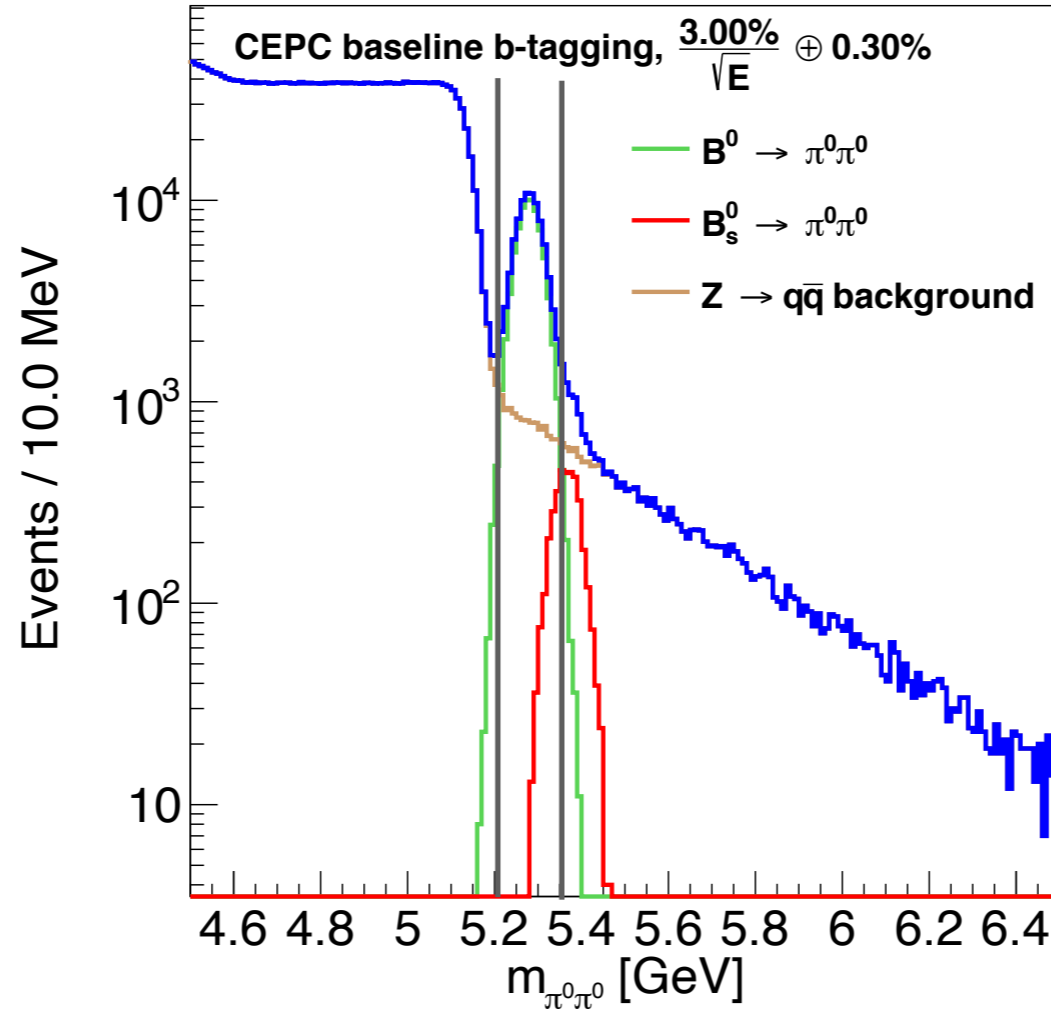
(a) Energy spectrum of π^0 pairs in $B^0 \rightarrow \pi^0\pi^0$ (left), $B_s^0 \rightarrow \pi^0\pi^0$ (middle), and $Z \rightarrow q\bar{q}$ (right) events.



(b) $\theta_{\pi^0\pi^0}$ vs $E_{\pi^0\pi^0}$ in $B^0 \rightarrow \pi^0\pi^0$ (left), $B_s^0 \rightarrow \pi^0\pi^0$ (middle), and $Z \rightarrow q\bar{q}$ (right) events.

Cut chain	$B^0 \rightarrow \pi^0\pi^0$	$B_s^0 \rightarrow \pi^0\pi^0$	$q\bar{q}$	$u\bar{u}+d\bar{d}+s\bar{s}$	$c\bar{c}$	$b\bar{b}$	$\sqrt{S} + B/S$
Total generated	191113	8948	7e11	4.285e11	1.203e11	1.512e11	
b-tagging ($\epsilon_{b,c,uds \rightarrow b} = 80\%, 8.26\%, 0.85\%$)	152890	7158	1.34539e11	3.64225e9	9.93678e9	1.2096e11	
$\pi^0 \rightarrow \gamma\gamma$	147932	6959	134272699126	3605151069	9908563142	120758984915	
Lower $E_{\pi^0} > 6$ GeV	92172	4396	15490570779	843830534	1598643569	13048096676	
Higher $E_{\pi^0} > 14$ GeV	87057	4148	2534286670	307734259	314762436	1911789975	
$E_{\pi^0\pi^0} > 22$ GeV	86807	4133	2233308564	289771547	281656846	1661880170	
$\theta_{\pi^0\pi^0} < 23^\circ$	77626	3644	825367542	119076559	102055313	604235671	
$m_{\pi^0\pi^0} \in (5.2188, 5.3405)$ GeV ($2.0 \sigma_{m_{B^0}} = 2.0 \times 0.0304$ GeV)	75374	717	17896	5640	1656	10600	0.4067% $\pm 0.0106\%$
$m_{\pi^0\pi^0} \in (5.3421, 5.3917)$ GeV ($0.8 \sigma_{m_{B_s^0}} = 0.8 \times 0.0310$ GeV)	3769	2394	5477	2400	507	2570	4.5070% $\pm 0.5563\%$

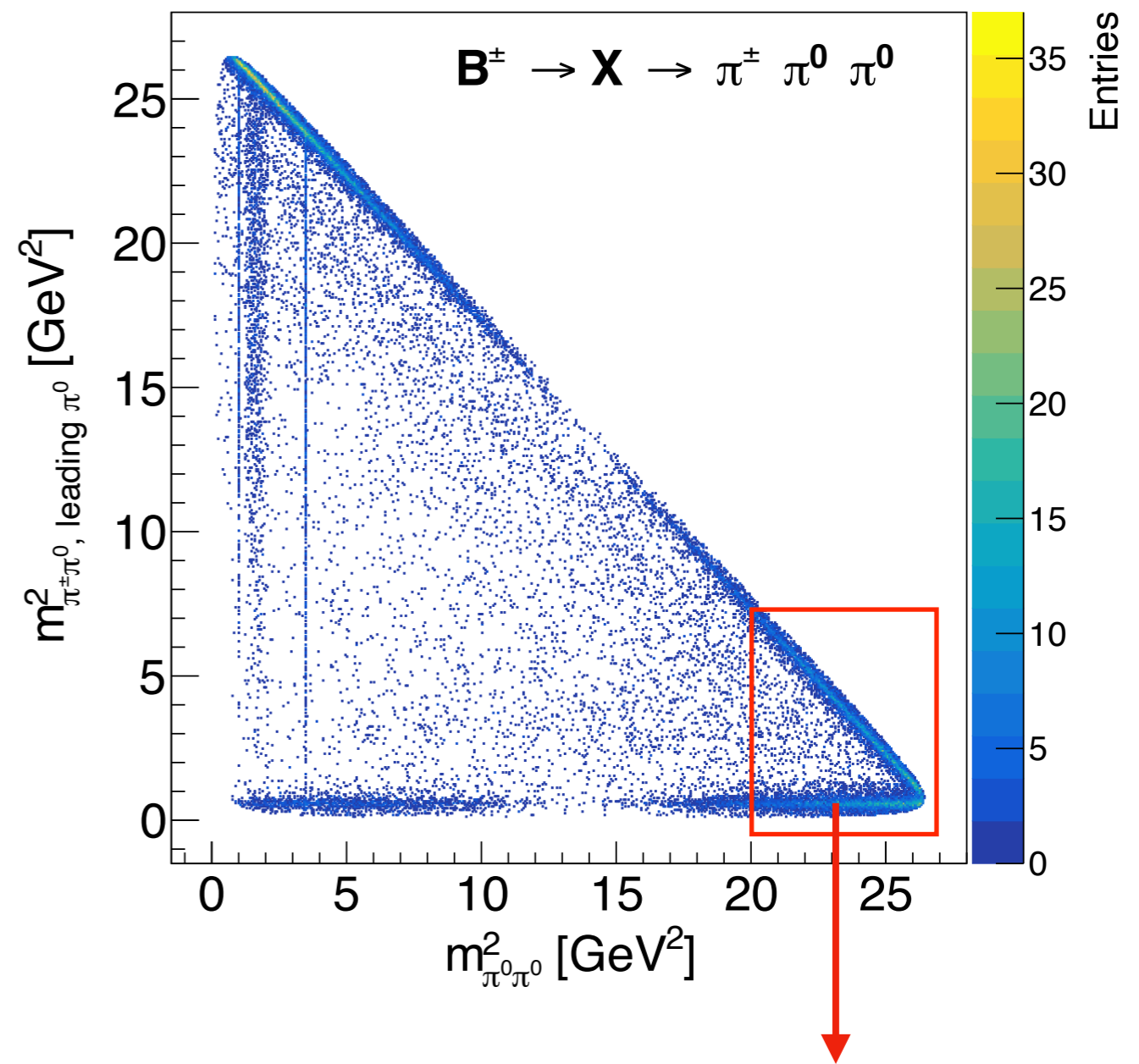
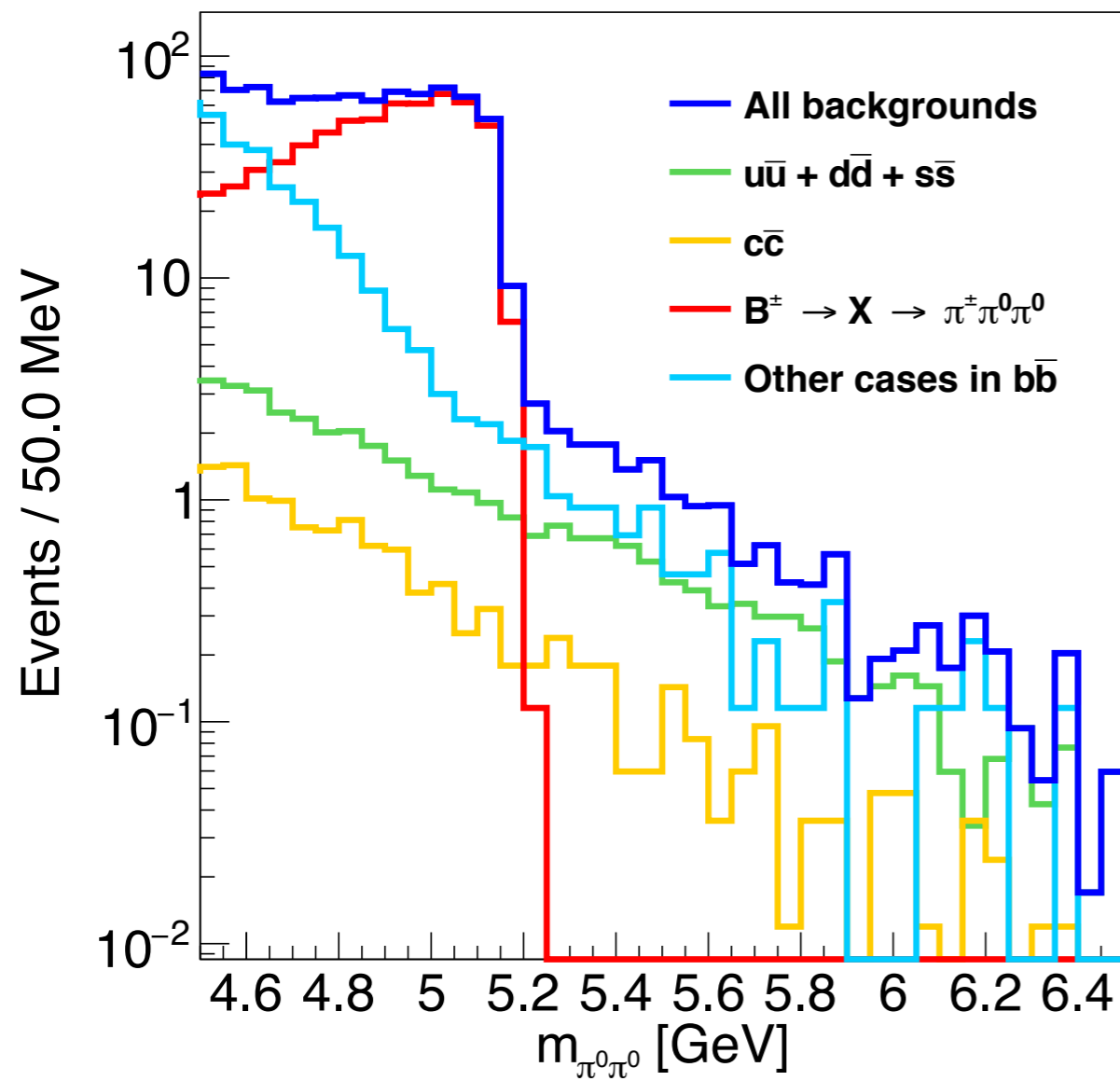
Event Selection



Cut chain	$B^0 \rightarrow \pi^0\pi^0$	$B_s^0 \rightarrow \pi^0\pi^0$	$q\bar{q}$	$u\bar{u}+d\bar{d}+s\bar{s}$	$c\bar{c}$	$b\bar{b}$	$\sqrt{S + B/S}$
Total generated	191113	8948	7e11	4.285e11	1.203e11	1.512e11	
b-tagging ($\epsilon_{b,c,uds \rightarrow b} = 80\%, 8.26\%, 0.85\%$)	152890	7158	1.34539e11	3.64225e9	9.93678e9	1.2096e11	
$\pi^0 \rightarrow \gamma\gamma$	147932	6959	134272699126	3605151069	9908563142	120758984915	
Lower $E_{\pi^0} > 6$ GeV	92172	4396	15490570779	843830534	1598643569	13048096676	
Higher $E_{\pi^0} > 14$ GeV	87057	4148	2534286670	307734259	314762436	1911789975	
$E_{\pi^0\pi^0} > 22$ GeV	86807	4133	2233308564	289771547	281656846	1661880170	
$\theta_{\pi^0\pi^0} < 23^\circ$	77626	3644	825367542	119076559	102055313	604235671	
$m_{\pi^0\pi^0} \in (5.2188, 5.3405)$ GeV ($2.0 \sigma_{m_{B^0}} = 2.0 \times 0.0304$ GeV)	75374	717	17896	5640	1656	10600	0.4067% $\pm 0.0106\%$
$m_{\pi^0\pi^0} \in (5.3421, 5.3917)$ GeV ($0.8 \sigma_{m_{B_s^0}} = 0.8 \times 0.0310$ GeV)	3769	2394	5477	2400	507	2570	4.5070% $\pm 0.5563\%$

Optimized
mass
window

Background components



$\sim 93\% B^\pm \rightarrow \rho(770)^\pm \pi^0, \rho(770)^\pm \rightarrow \pi^\pm \pi^0$
 $\sim 7\% B^\pm \rightarrow \pi^\pm \pi^0 \pi^0$

Dependence on b-tagging performance

Three b-tagging conditions, at $3\%/\sqrt{E} \oplus 0.3\%$

Accuracy

$B^0 \rightarrow \pi^0 \pi^0$

b-tagging	Mass window (GeV)	$n \sigma_{m_B}$	$B^0 \rightarrow \pi^0 \pi^0$	$B_s^0 \rightarrow \pi^0 \pi^0$	$q\bar{q}$	$u\bar{u}+d\bar{d}+s\bar{s}$	$c\bar{c}$	$b\bar{b}$	$\sqrt{S+B}/S$
No b-tagging ($\epsilon_{b,c,uds \rightarrow b} = 100\%, 100\%, 100\%$)	(5.2370, 5.3222)	1.4	85986	311	517718	494139	15549	8030	0.9038% $\pm 0.0308\%$
CEPC baseline b-tagging ($\epsilon_{b,c,uds \rightarrow b} = 80\%, 8.26\%, 0.85\%$)	(5.2188, 5.3405)	2.0	75374	717	17896	5640	1656	10600	0.4067% $\pm 0.0106\%$
Ideal b-tagging ($\epsilon_{b,c,uds \rightarrow b} = 100\%, 0\%, 0\%$)	(5.2188, 5.3405)	2.0	94217	896	13250	0	0	13250	0.3494% $\pm 0.0047\%$

$B_s \rightarrow \pi^0 \pi^0$

b-tagging	Mass window (GeV)	$n \sigma_{m_B}$	$B^0 \rightarrow \pi^0 \pi^0$	$B_s^0 \rightarrow \pi^0 \pi^0$	$q\bar{q}$	$u\bar{u}+d\bar{d}+s\bar{s}$	$c\bar{c}$	$b\bar{b}$	$\sqrt{S+B}/S$
No b-tagging ($\epsilon_{b,c,uds \rightarrow b} = 100\%, 100\%, 100\%$)	(5.3328, 5.4010)	1.1	8563	3613	353469	338838	9411	5220	16.7354% $\pm 0.7580\%$
CEPC baseline b-tagging ($\epsilon_{b,c,uds \rightarrow b} = 80\%, 8.26\%, 0.85\%$)	(5.3421, 5.3917)	0.8	3769	2394	5477	2400	507	2570	4.5070% $\pm 0.5563\%$
Ideal b-tagging ($\epsilon_{b,c,uds \rightarrow b} = 100\%, 0\%, 0\%$)	(5.3421, 5.3917)	0.8	4712	2992	3212	0	0	3212	3.4917% $\pm 0.1953\%$

2~3 times

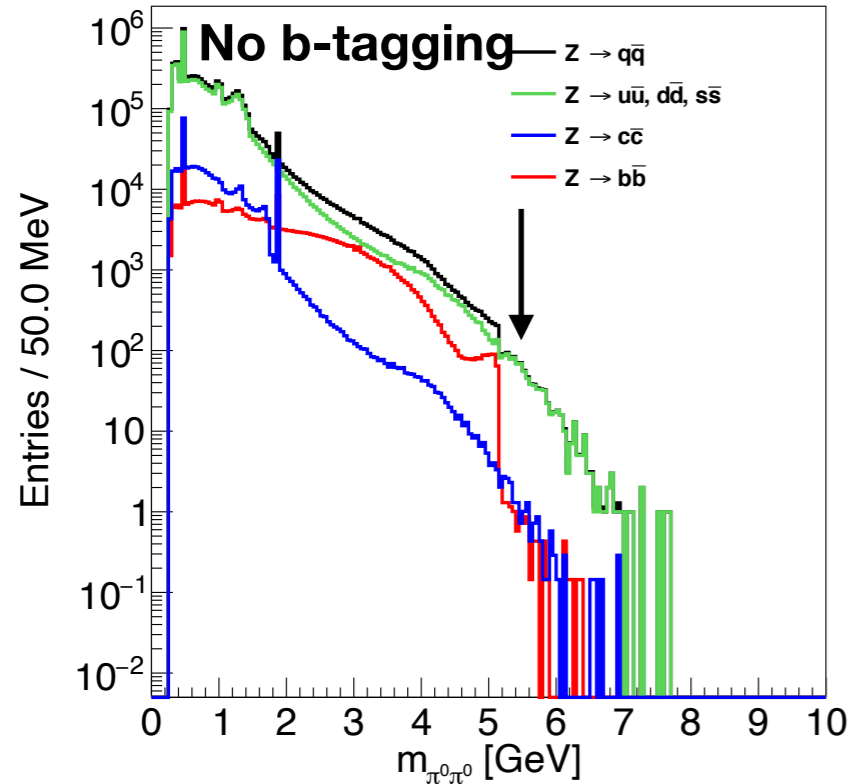
~1.2 times

comparable

No b-tagging \longrightarrow CEPC baseline b-tagging \longrightarrow Ideal b-tagging

Dependence on b-tagging performance

b-tagging is essential to reduce the hard combinatorial background in non-bb events



π^0 s in light-quark events (mainly from hadronization) are harder than those in cc and bb events (mainly from c and b hadrons)

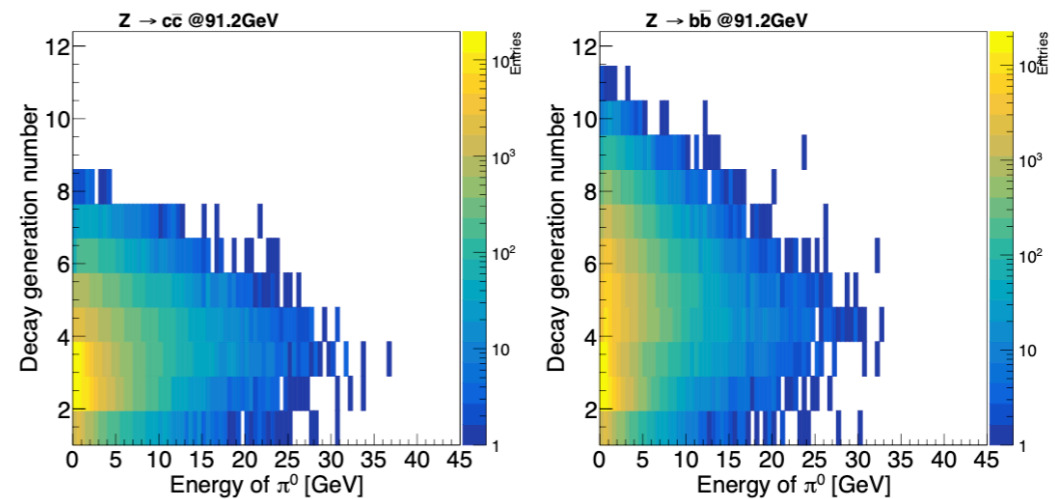
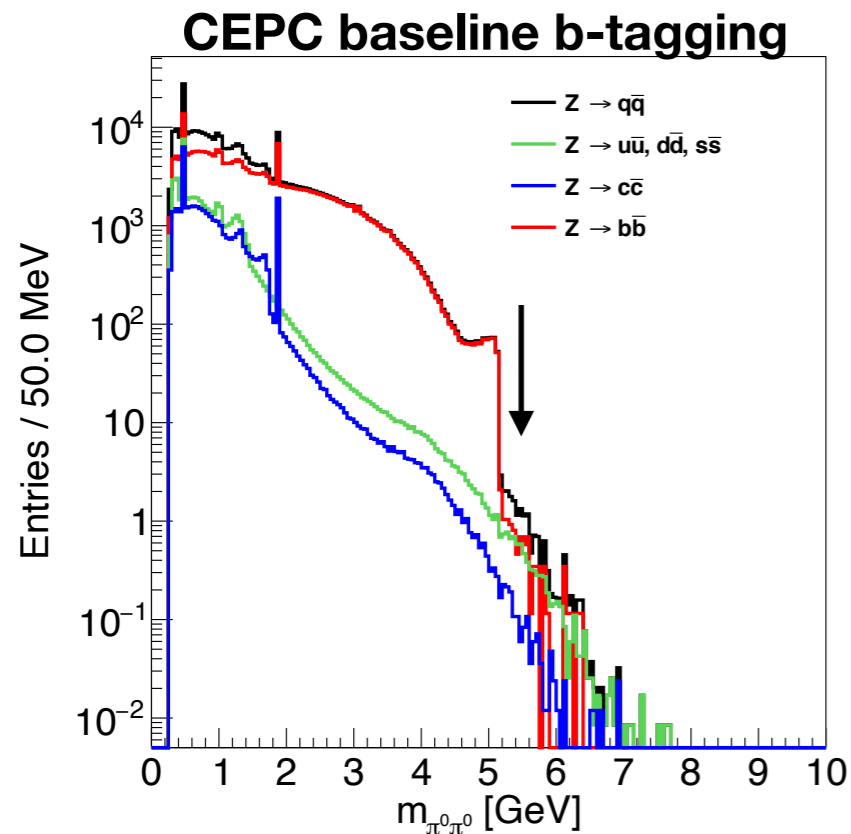
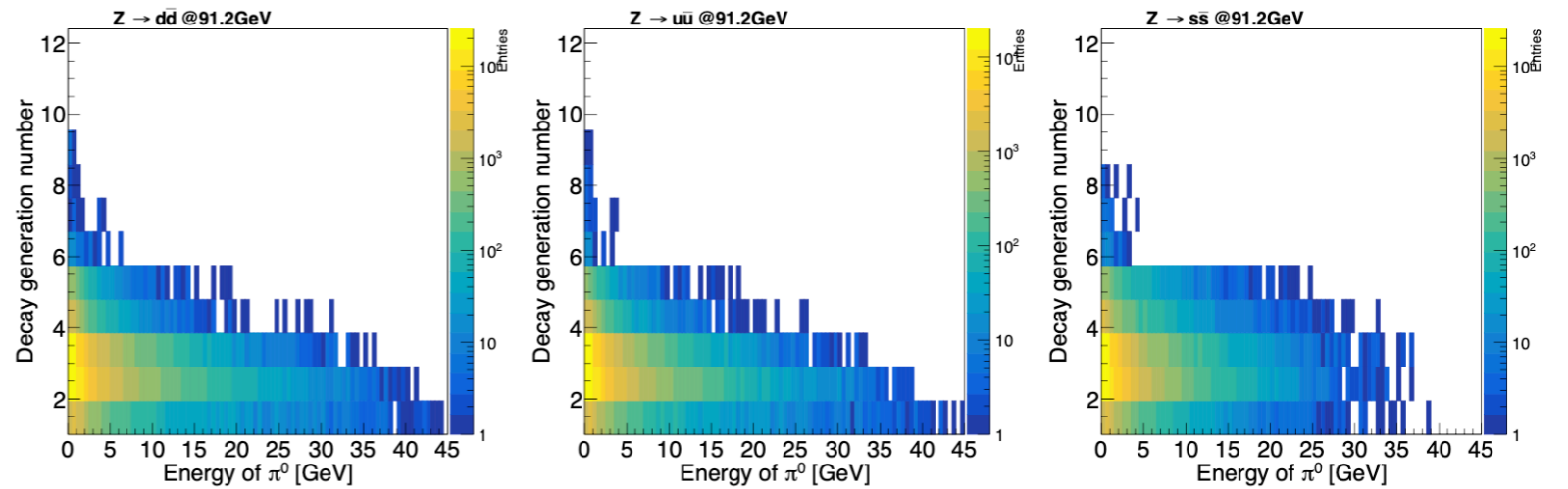
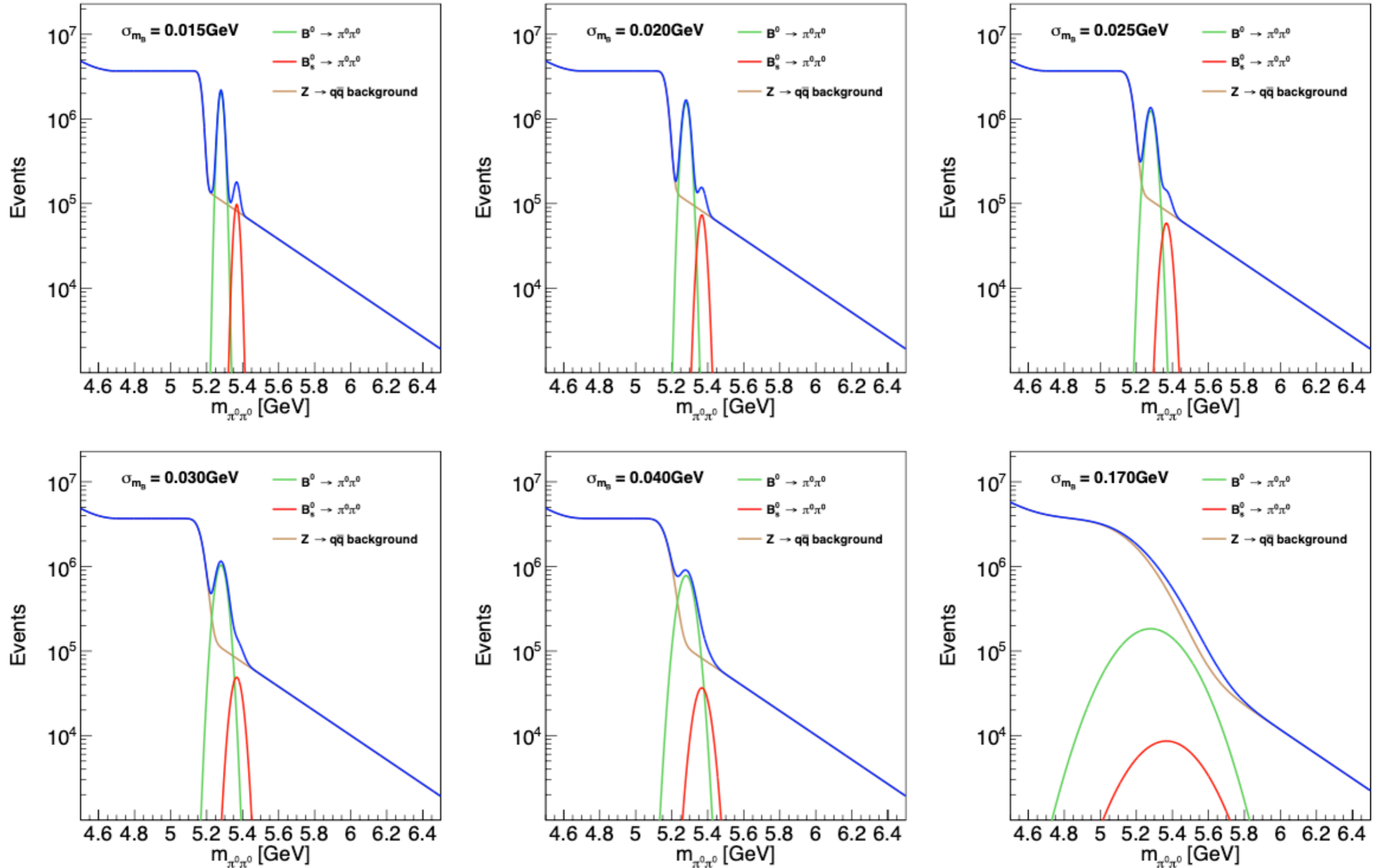


Figure 5: Decay generation number of π^0 vs E_{π^0} in $Z \rightarrow u\bar{u}$, $Z \rightarrow d\bar{d}$, $Z \rightarrow s\bar{s}$, $Z \rightarrow c\bar{c}$, $Z \rightarrow b\bar{b}$ events.

Dependence on B mass resolution

with CEPC baseline b-tagging



Dependence on B mass resolution

with CEPC baseline b-tagging

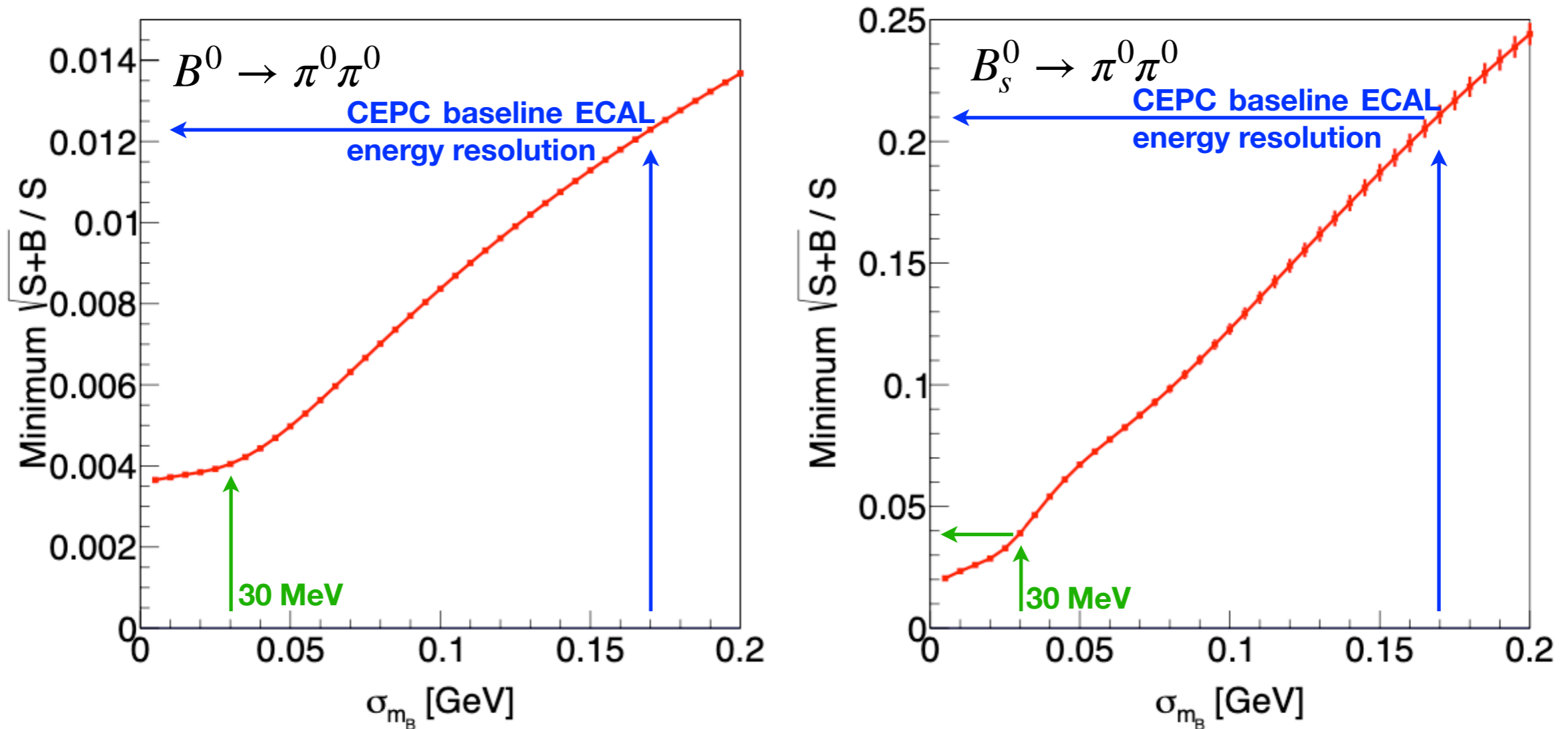


Figure 13: Accuracy of $B^0 \rightarrow \pi^0 \pi^0$ (left) and $B_s^0 \rightarrow \pi^0 \pi^0$ (right) vs σ_{m_B} (GeV).

- CEPC baseline ECAL energy resolution $\sim 17\%/\sqrt{E} \oplus 1\%$

Summary

$B^0_{(s)} \rightarrow \pi^0\pi^0$ are important to understand

- $B^0 \rightarrow \pi^0\pi^0$: CKM angle α and $B \rightarrow \pi\pi$ puzzle
- $B^0_s \rightarrow \pi^0\pi^0$: annihilation mechanism

Fast Simulation is used to study the dependence of $B^0_{(s)} \rightarrow \pi^0\pi^0$ accuracy on

❖ b-tagging:

- essential to reduce the hard combinatorial background in non-bb events

Accuracy at $3\%/\sqrt{E} \oplus 1\%$	$B^0 \rightarrow \pi^0\pi^0$	$B^0_s \rightarrow \pi^0\pi^0$	
No b-tagging	0.9%	16.7%	↓ 2~3 times improvement
CEPC baseline b-tagging	0.4%	4.5%	

❖ B mass resolution (σ_{mB}):

- 2σ separation of B^0 and B^0_s requires σ_{mB} better than 30 MeV ($\sim 3\%/\sqrt{E} \oplus 0.3\%$).

Accuracy with CEPC baseline b-tagging	$B^0 \rightarrow \pi^0\pi^0$	$B^0_s \rightarrow \pi^0\pi^0$	
$17\%/\sqrt{E} \oplus 1\%$ (CEPC baseline)	$\sim 1.2\%$	$\sim 21\%$	↓ 3~5 times improvement
$3\%/\sqrt{E} \oplus 0.3\%$ ($\sigma_{mB} \sim 30$ MeV)	$\sim 0.4\%$	$\sim 4\%$	

👉 Need to further understand and estimate the corresponding improvement on the CKM- α measurement...

Thanks!

Backup

CKM Quark-Mixing Matrix

12.3 Phases of CKM elements

As can be seen from Fig. 12.1, the angles of the unitarity triangle are

$$\begin{aligned}\beta = \phi_1 &= \arg\left(-\frac{V_{cd}V_{cb}^*}{V_{td}V_{tb}^*}\right), \\ \alpha = \phi_2 &= \arg\left(-\frac{V_{td}V_{tb}^*}{V_{ud}V_{ub}^*}\right), \\ \gamma = \phi_3 &= \arg\left(-\frac{V_{ud}V_{ub}^*}{V_{cd}V_{cb}^*}\right).\end{aligned}\quad (12.16)$$

Since CP violation involves phases of CKM elements, many measurements of CP -violating observables can be used to constrain these angles and the $\bar{\rho}, \bar{\eta}$ parameters.

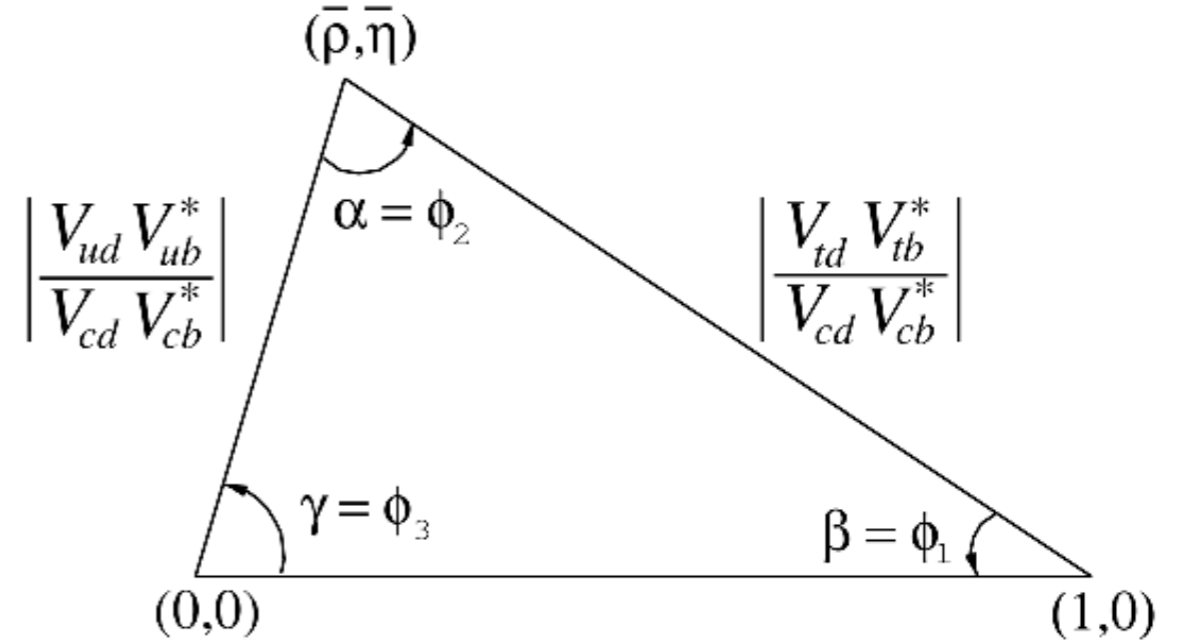


Figure 12.1: Sketch of the unitarity triangle.

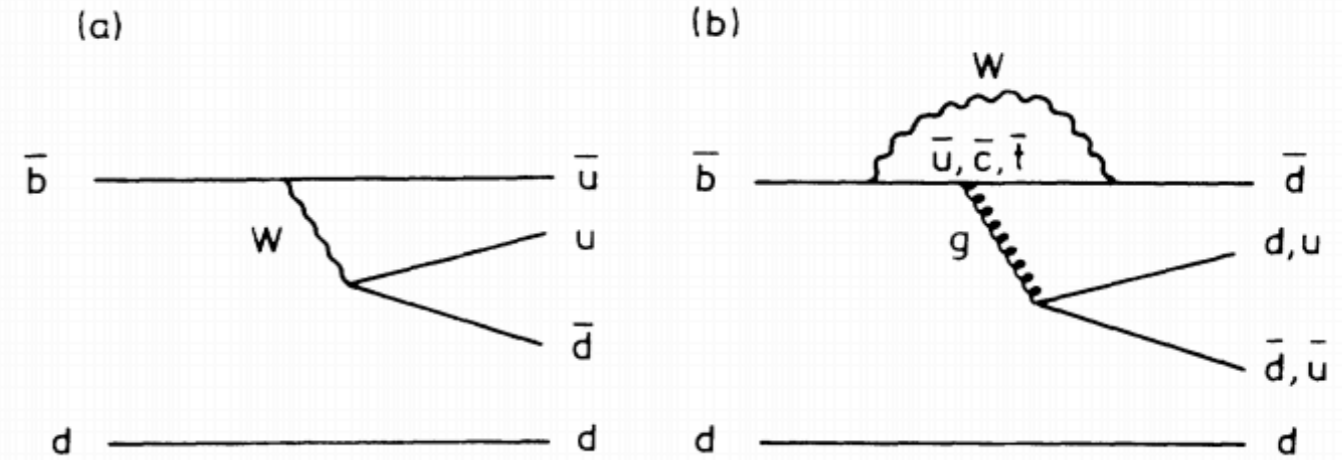
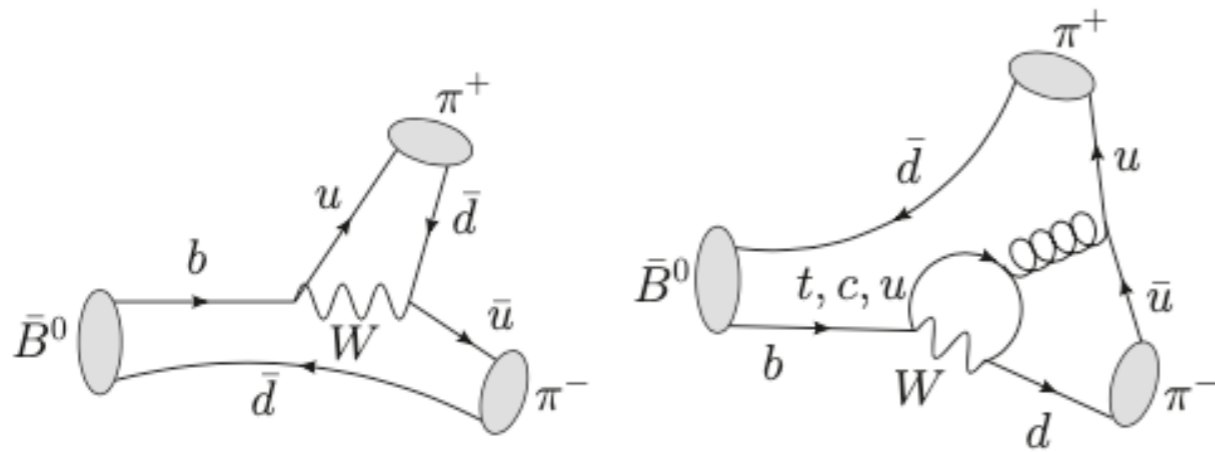
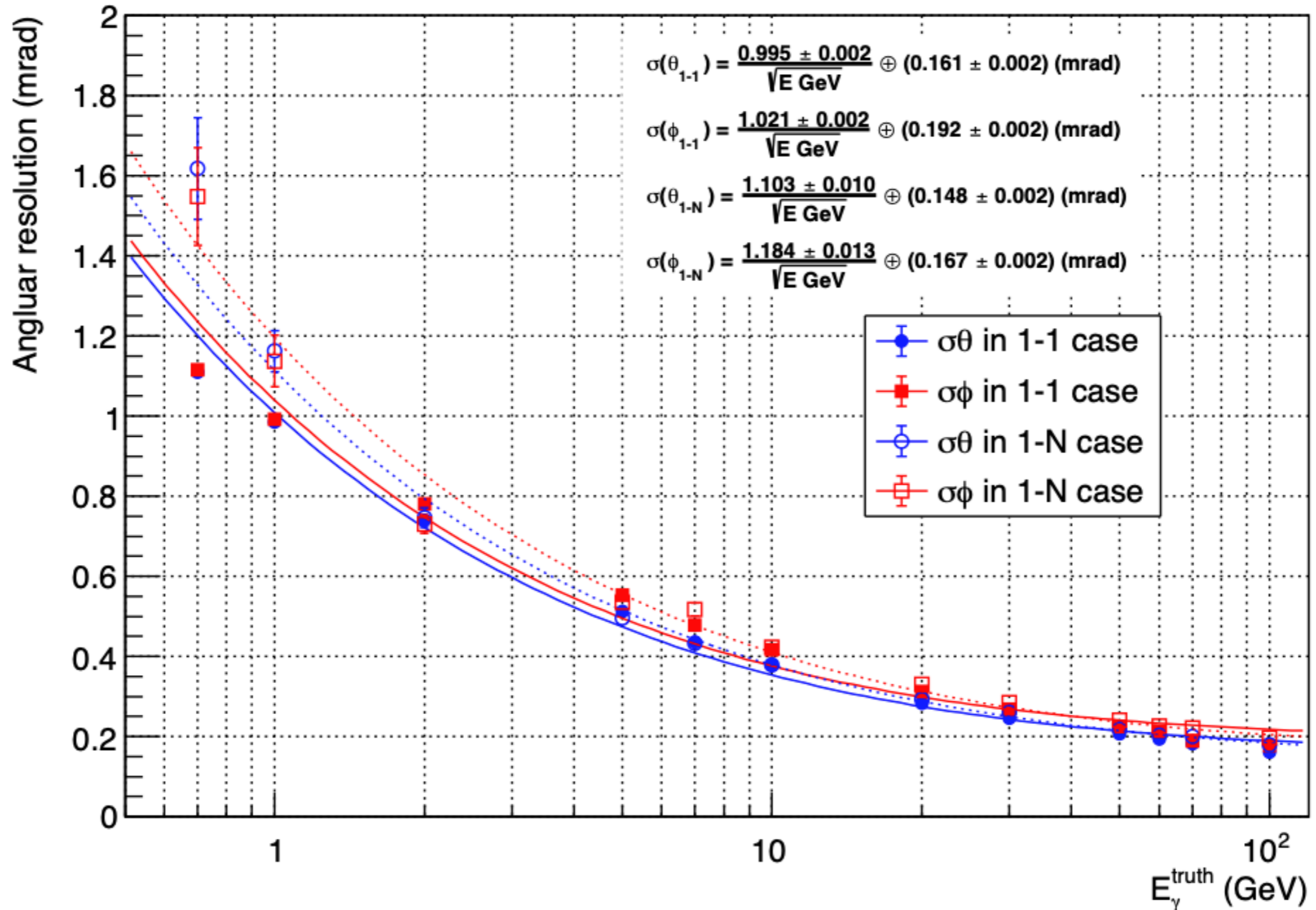


FIG. 1. (a) Tree-level and (b) penguin diagrams for the decay $B_d^0 \rightarrow \pi\pi$.

Single photon angular resolution

CEPC baseline full simulation results by Yuzhi



Efficiency induced by di-photon merging

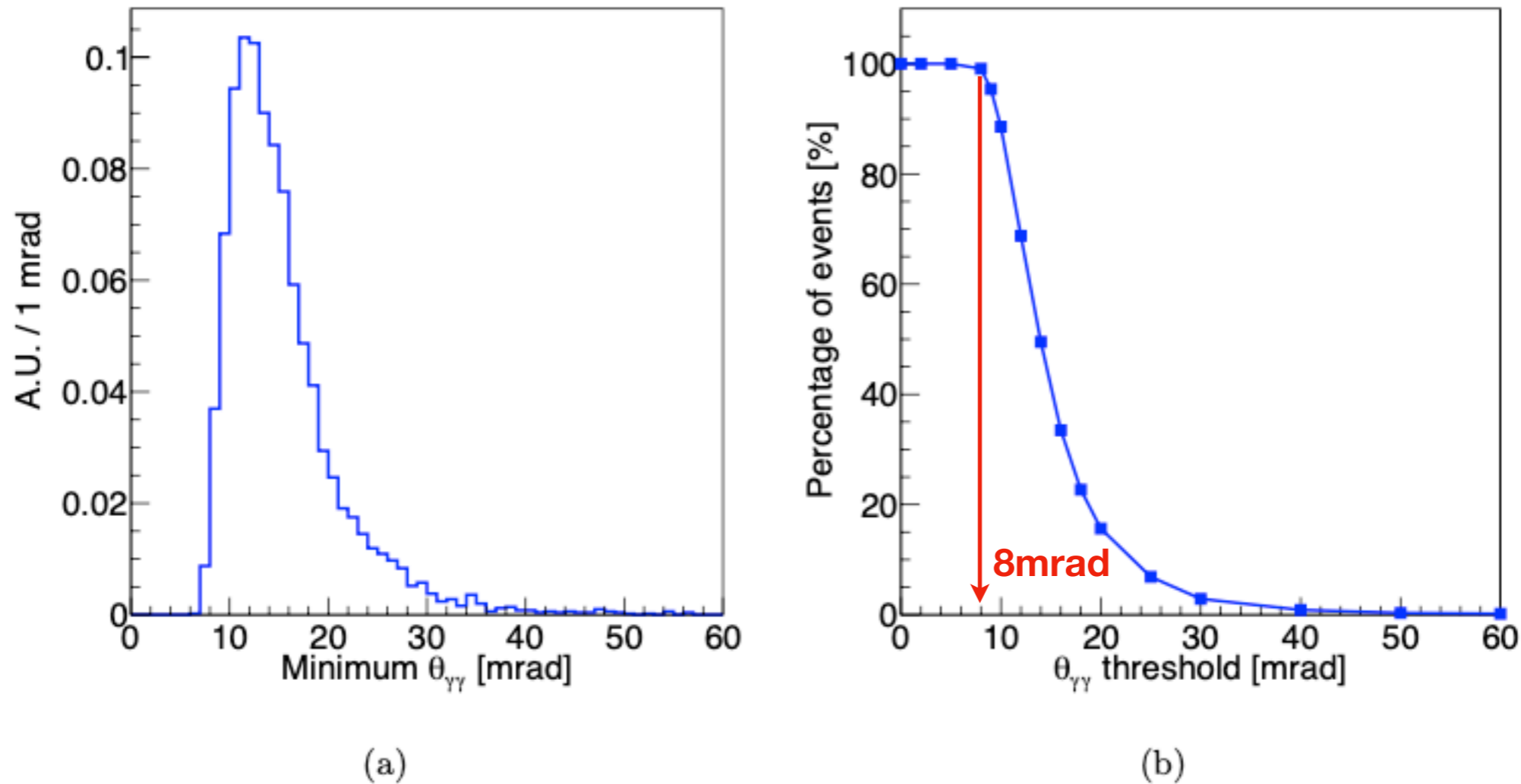


Figure 2: (a) Distribution of the minimum opening angle among 4 photons from $B_{(s)}^0 \rightarrow \pi^0 \pi^0$. (b) Percentage of $B_{(s)}^0 \rightarrow \pi^0 \pi^0$ signal events with minimum $\theta_{\gamma\gamma}$ over different $\theta_{\gamma\gamma}$ thresholds.

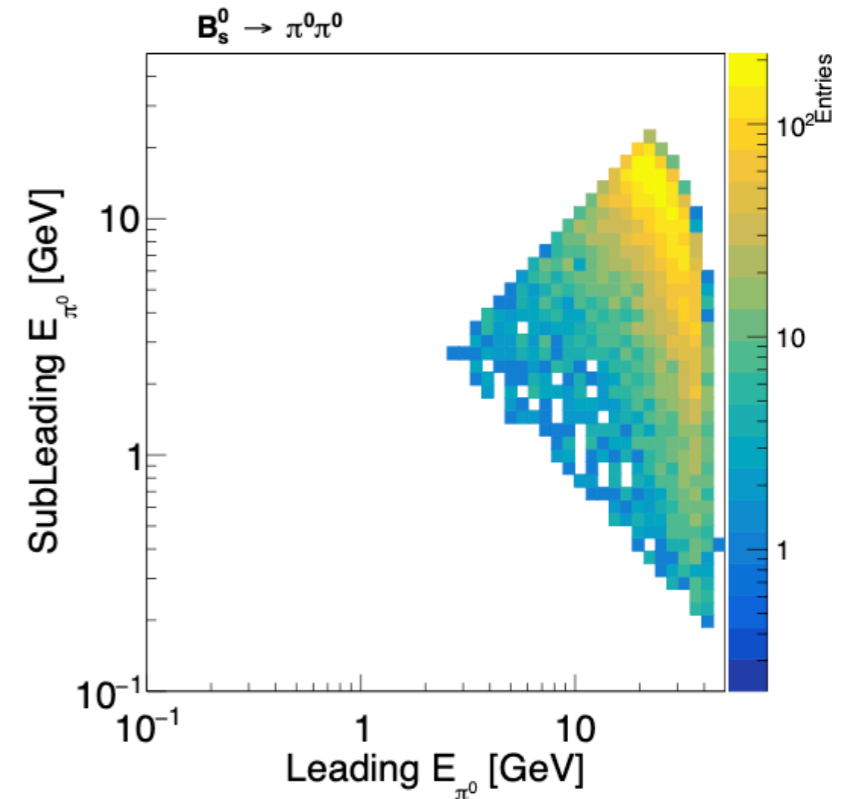
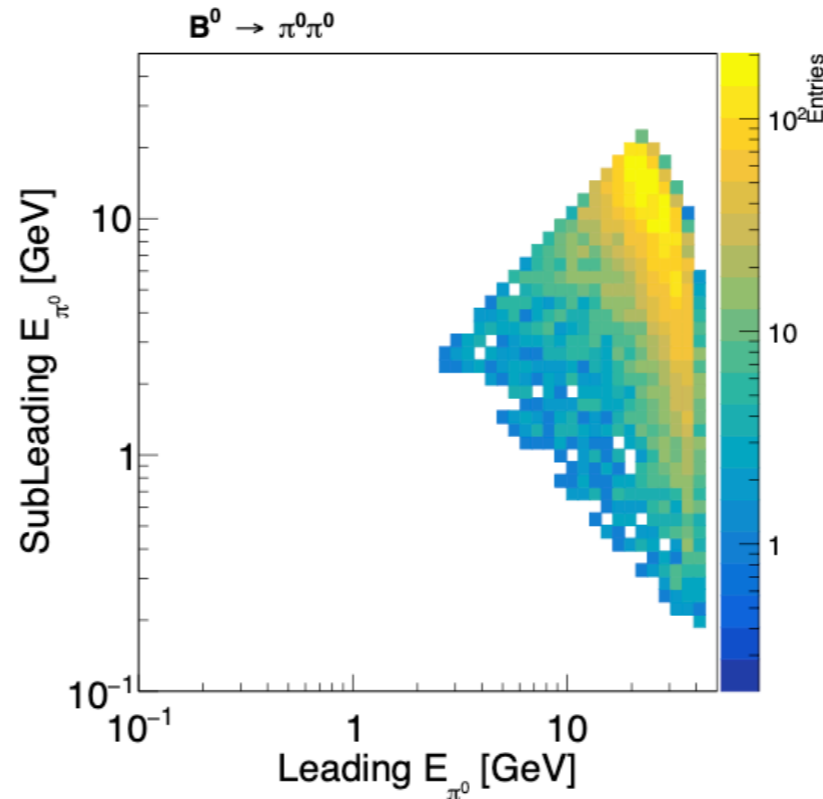
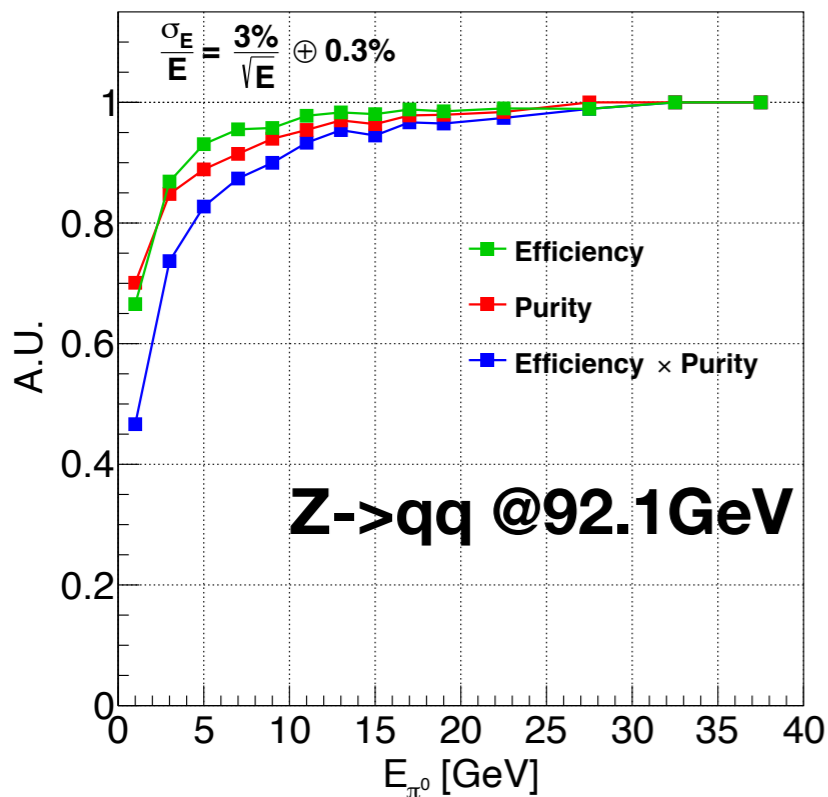
For radius = 1800 mm:

8 mrad ~ 14.4 mm separation distance, 100% efficiency.

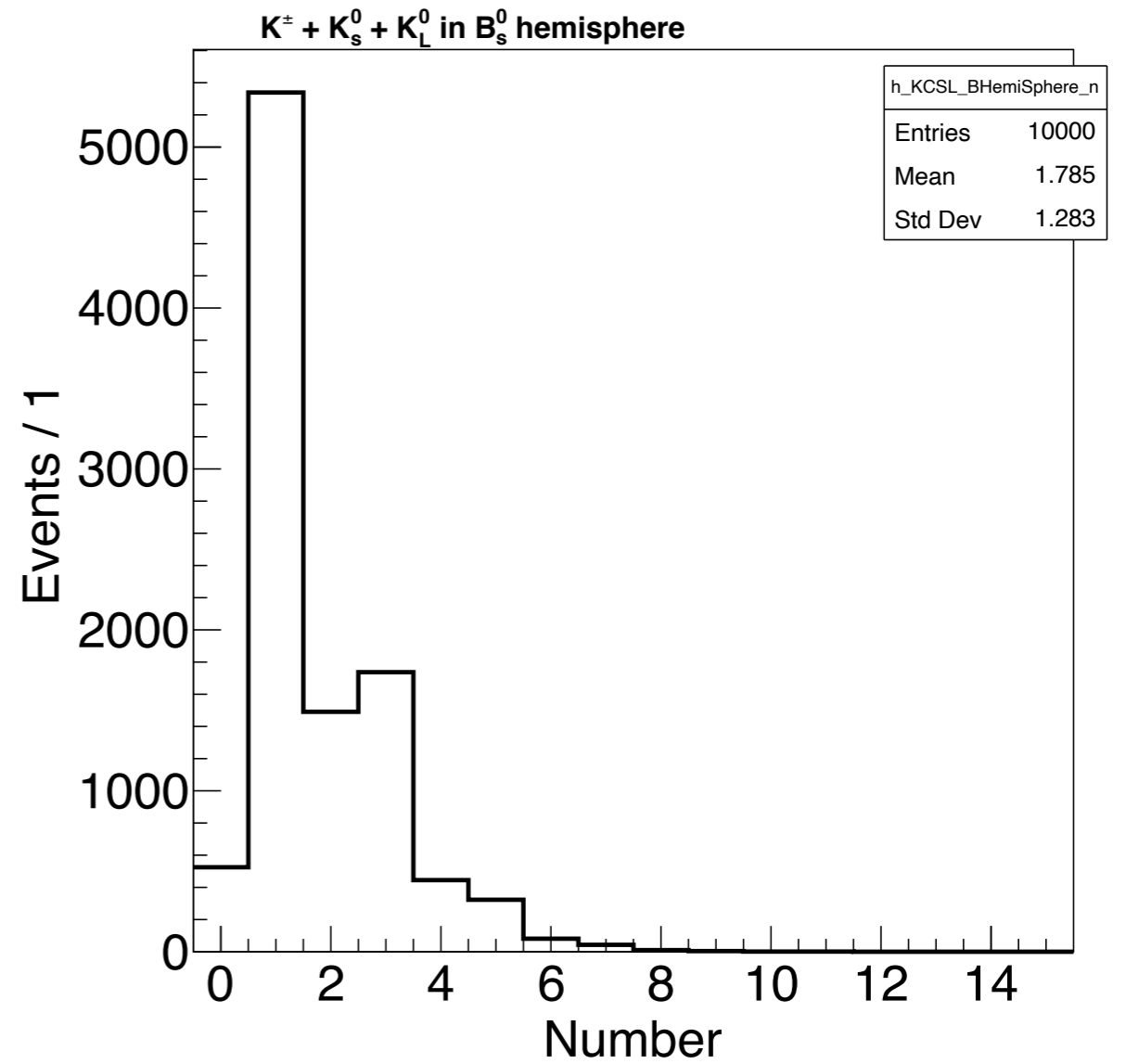
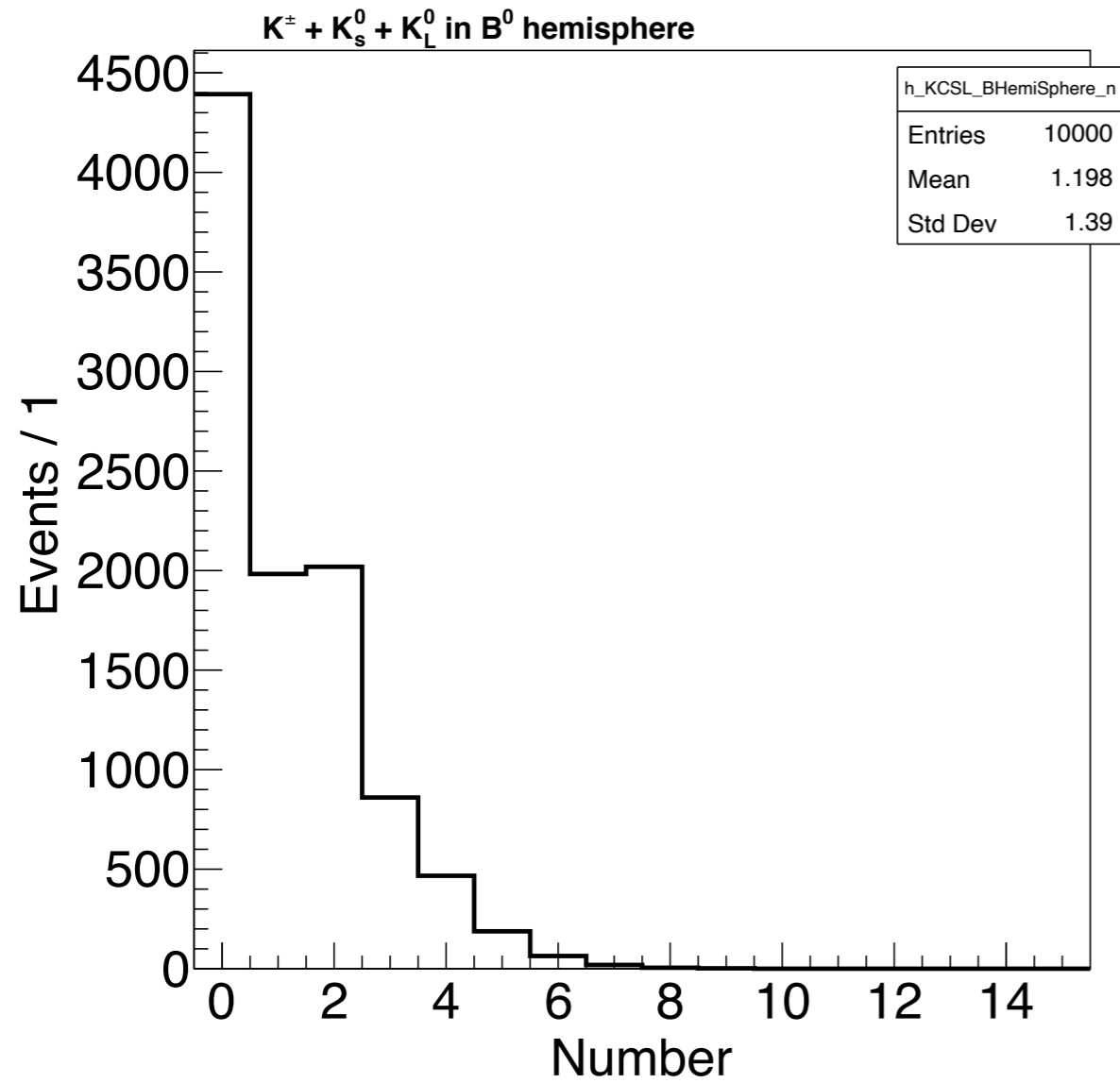
11 mrad ~ 20 mm, ~10% efficiency lost, accuracy is degraded by 10% at most.

Event Selection

Cut chain	$B^0 \rightarrow \pi^0\pi^0$	$B_s^0 \rightarrow \pi^0\pi^0$	$q\bar{q}$	$u\bar{u}+d\bar{d}+s\bar{s}$	$c\bar{c}$	$b\bar{b}$	$\sqrt{S+B}/S$
Total generated	191113	8948	7e11 (100.00%)	4.285e11 (61.21%)	1.203e11 (17.19%)	1.512e11 (21.60%)	
b-tagging ($\epsilon_{b,c,uds \rightarrow b} = 80\%, 8.26\%, 0.85\%$)	152890	7158	1.34539e11 (100.00%)	3.64225e9 (2.70%)	9.93678e9 (7.38%)	1.2096e11 (89.92%)	
$\pi^0 \rightarrow \gamma\gamma$	147932	6959	134272699126	3605151069	9908563142	120758984915	
Lower $E_{\pi^0} > 6$ GeV	92172	4396	15490570779	843830534	1598643569	13048096676	
Higher $E_{\pi^0} > 14$ GeV	87057	4148	2534286670	307734259	314762436	1911789975	
$E_{\pi^0\pi^0} > 22$ GeV	86807	4133	2233308564	289771547	281656846	1661880170	
$\theta_{\pi^0\pi^0} < 23^\circ$	77626	3644	825367542	119076559	102055313	604235671	
$m_{\pi^0\pi^0} \in (5.2188, 5.3405)$ GeV ($2.0 \sigma_{m_{B^0}} = 2.0 \times 0.0304$ GeV)	75374	717	17896	5640	1656	10600	0.4067% $\pm 0.0106\%$
$m_{\pi^0\pi^0} \in (5.3421, 5.3917)$ GeV ($0.8 \sigma_{m_{B_s^0}} = 0.8 \times 0.0310$ GeV)	3769	2394	5477	2400	507	2570	4.5070% $\pm 0.5563\%$



Leading kaon in B meson hemisphere



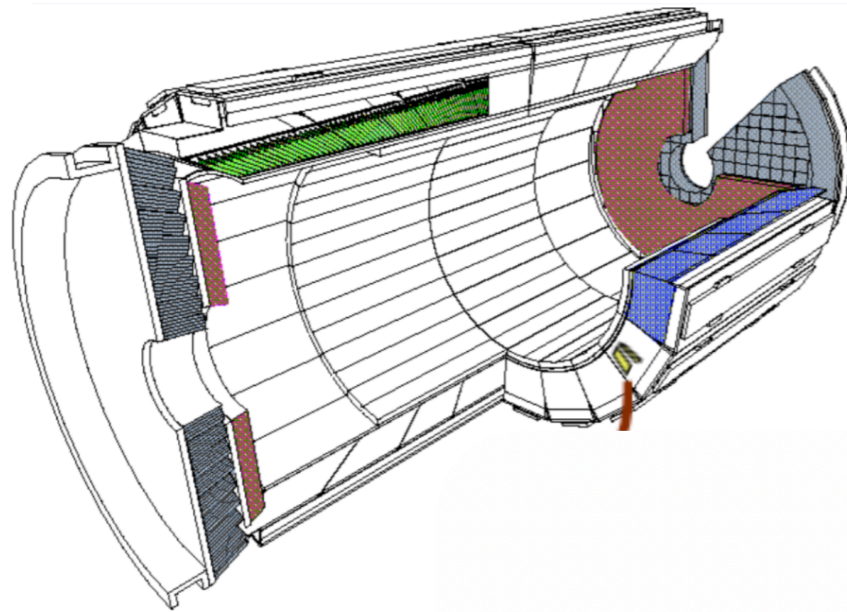
Results at a benchmark detector setup

A **benchmark** detector setup for $B^0_{(s)} \rightarrow \pi^0\pi^0$ measurement

ECAL energy resolution

$$3\% \sqrt{E} \oplus 0.3\%$$

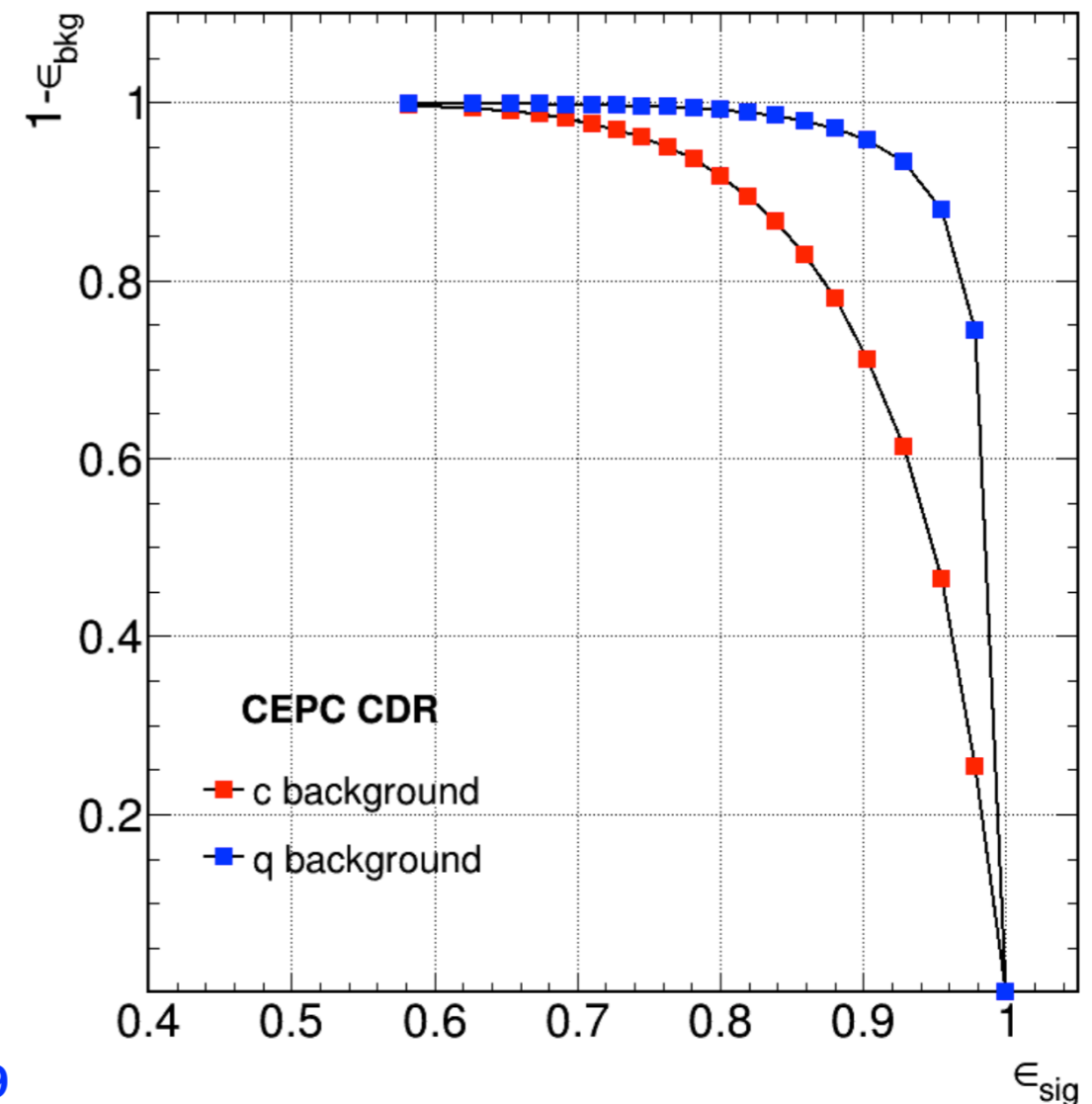
LHC - CMS (PbWO₄)



$$\frac{\sigma_E}{E} = \frac{2.8\%}{\sqrt{E(\text{GeV})}} \oplus \frac{12\%}{E(\text{GeV})} \oplus 0.3\%$$

b-tagging

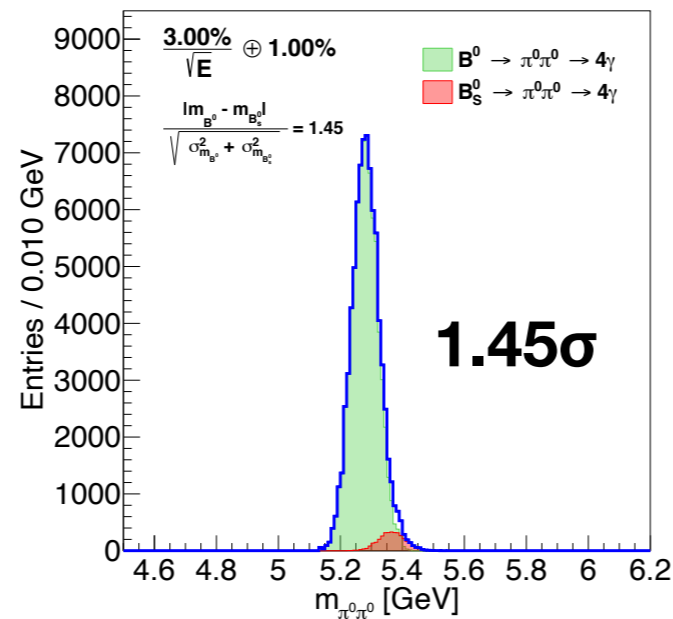
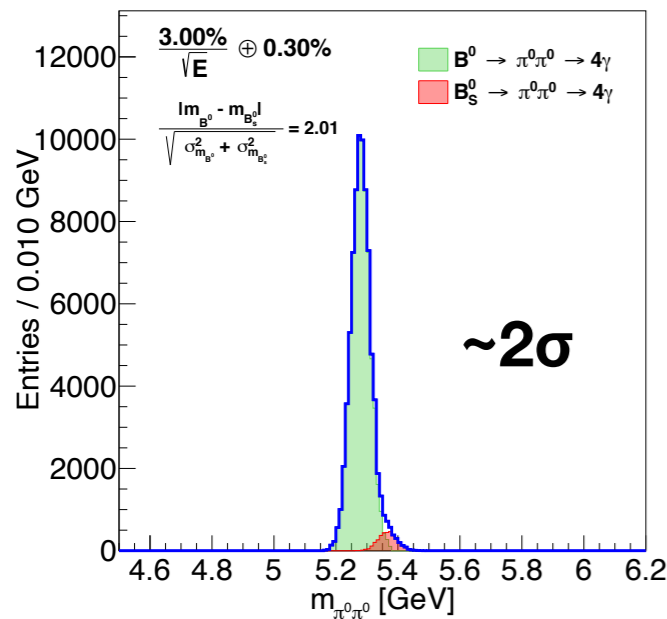
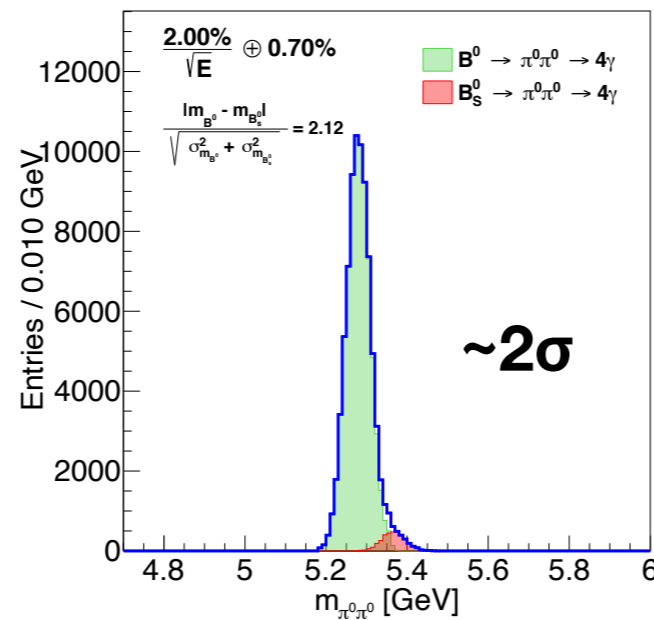
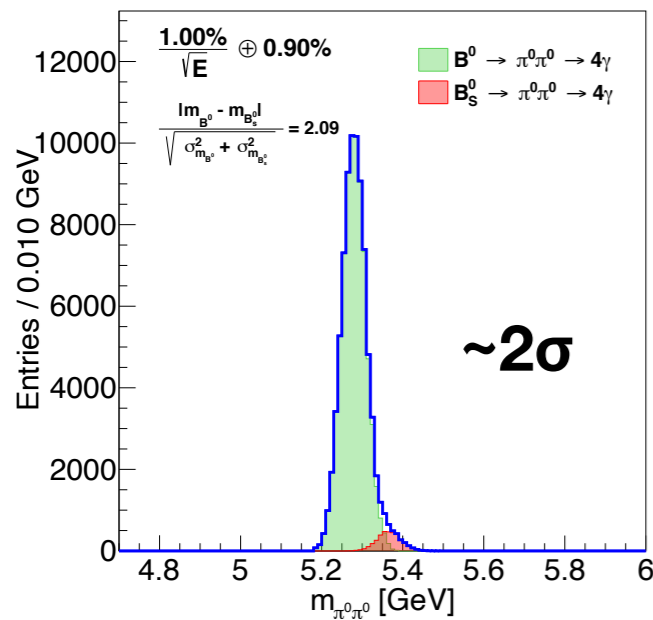
CEPC baseline b-tagging
80% efficiency and 90% purity



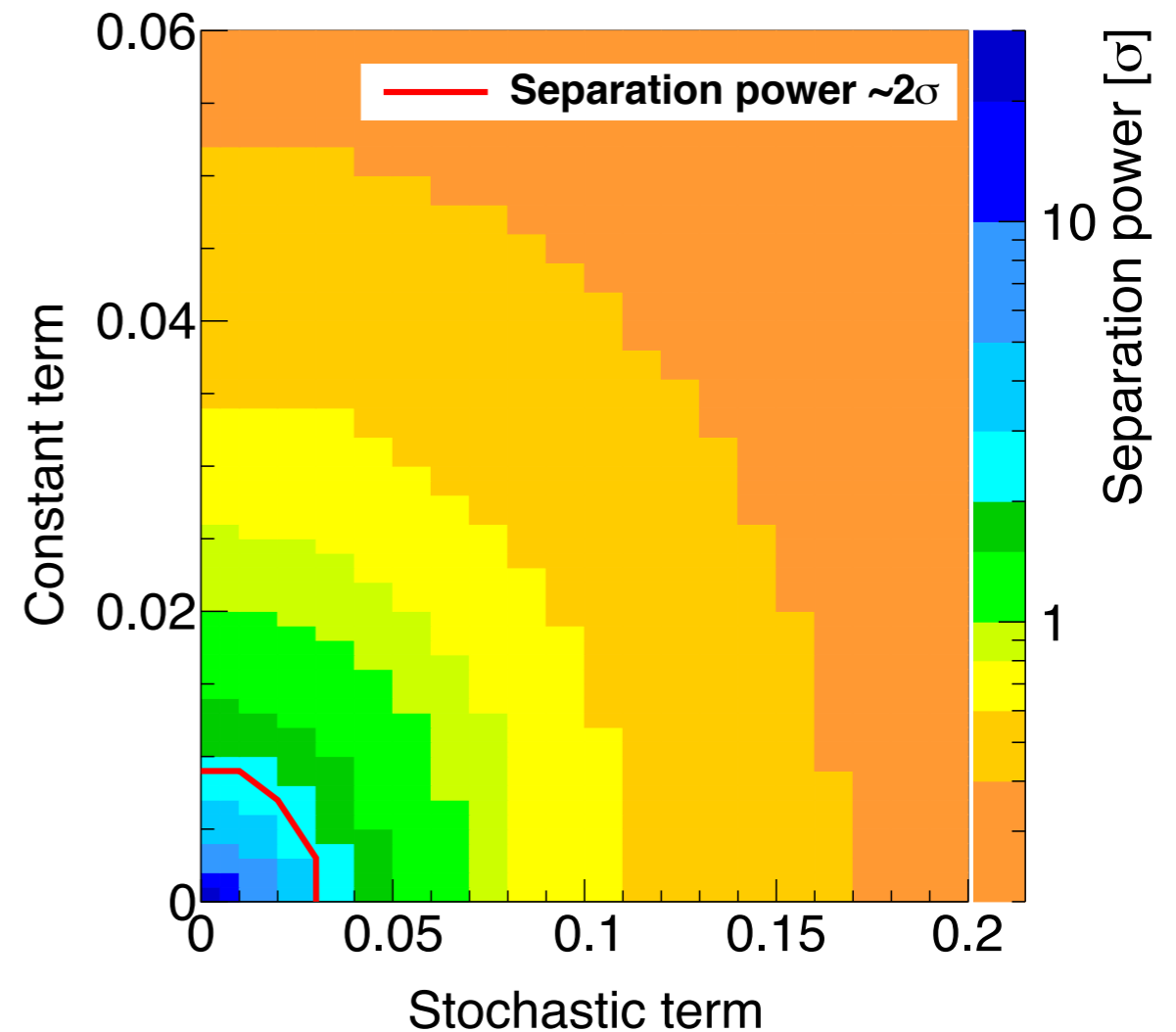
Separation of B^0 and B_s

$$m_{B^0} = 5279.63 \pm 0.15 \text{ MeV}$$

$$m_{B_s^0} = 5366.89 \pm 0.19 \text{ MeV}$$



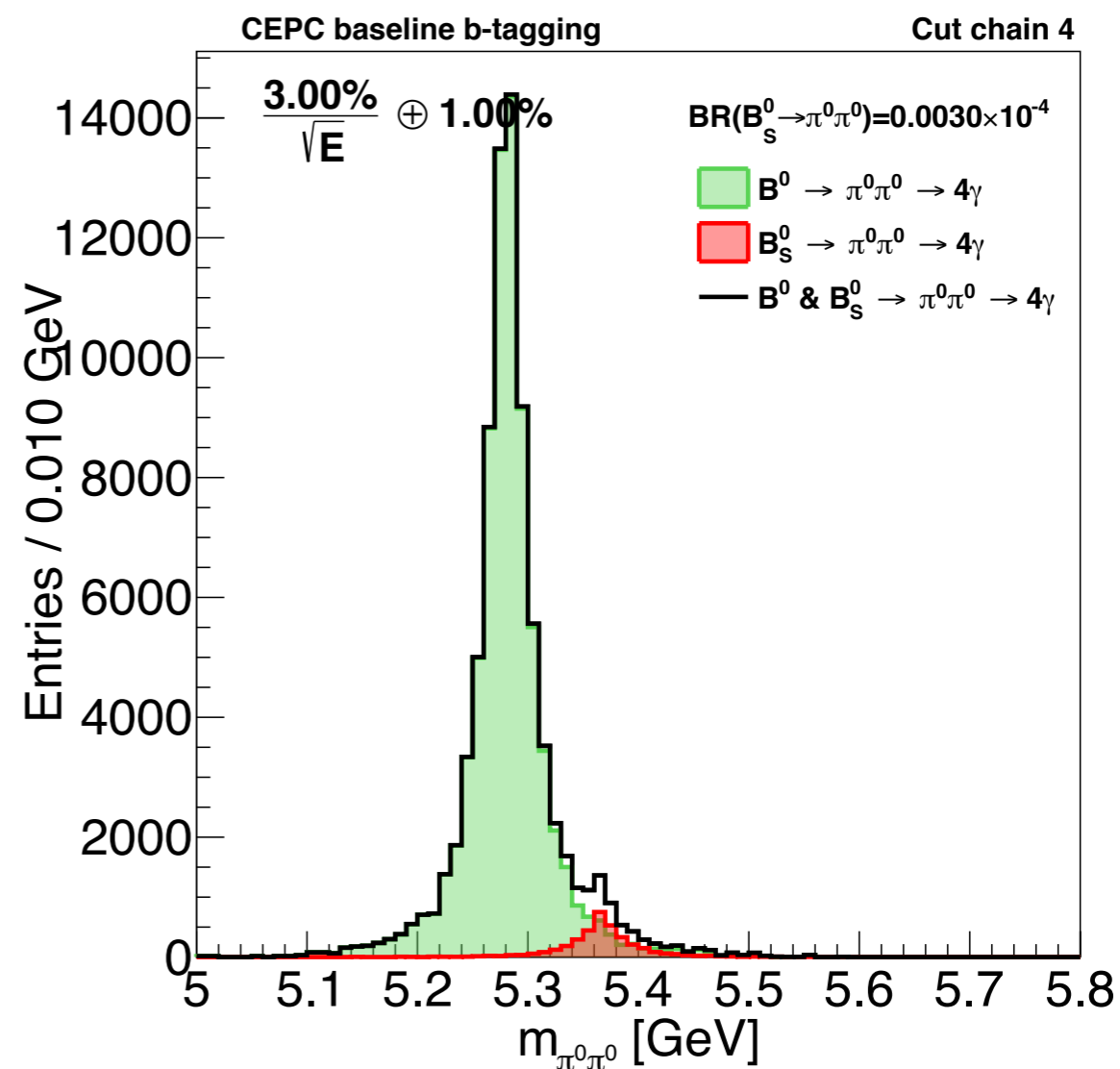
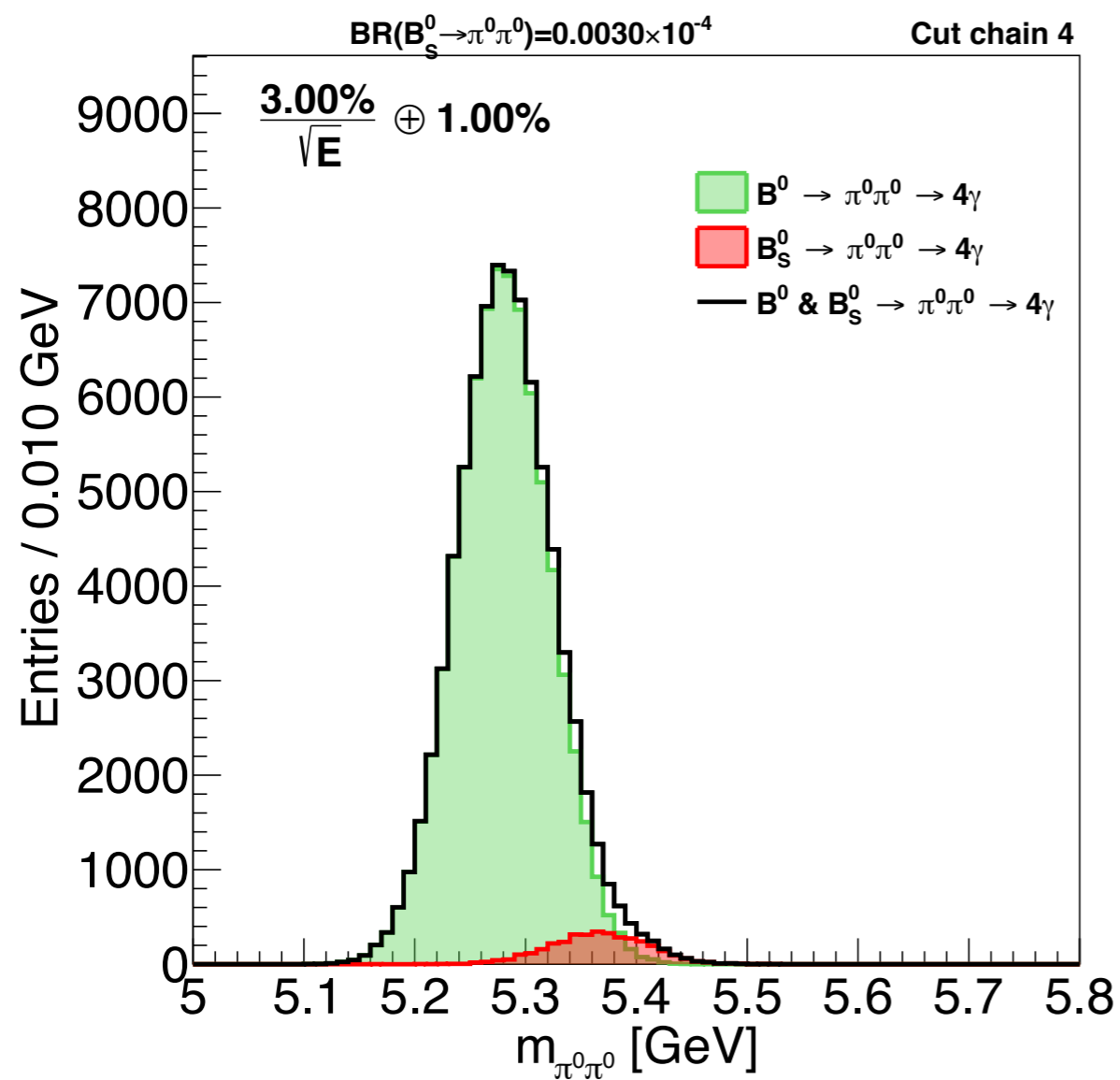
$$\text{separation power} = \frac{|m_{B^0} - m_{B_s^0}|}{\sqrt{\sigma_{m_{B^0}}^2 + \sigma_{m_{B_s^0}}^2}}$$



A 2σ separation requires ECAL energy resolution **better than $3\%/\sqrt{E} \oplus 0.3\%$**

Kinematic Fit

at $3\%/\sqrt{E} \oplus 1\%$ ECAL resolution



Signal peak gets sharpened after Kinematic Fit

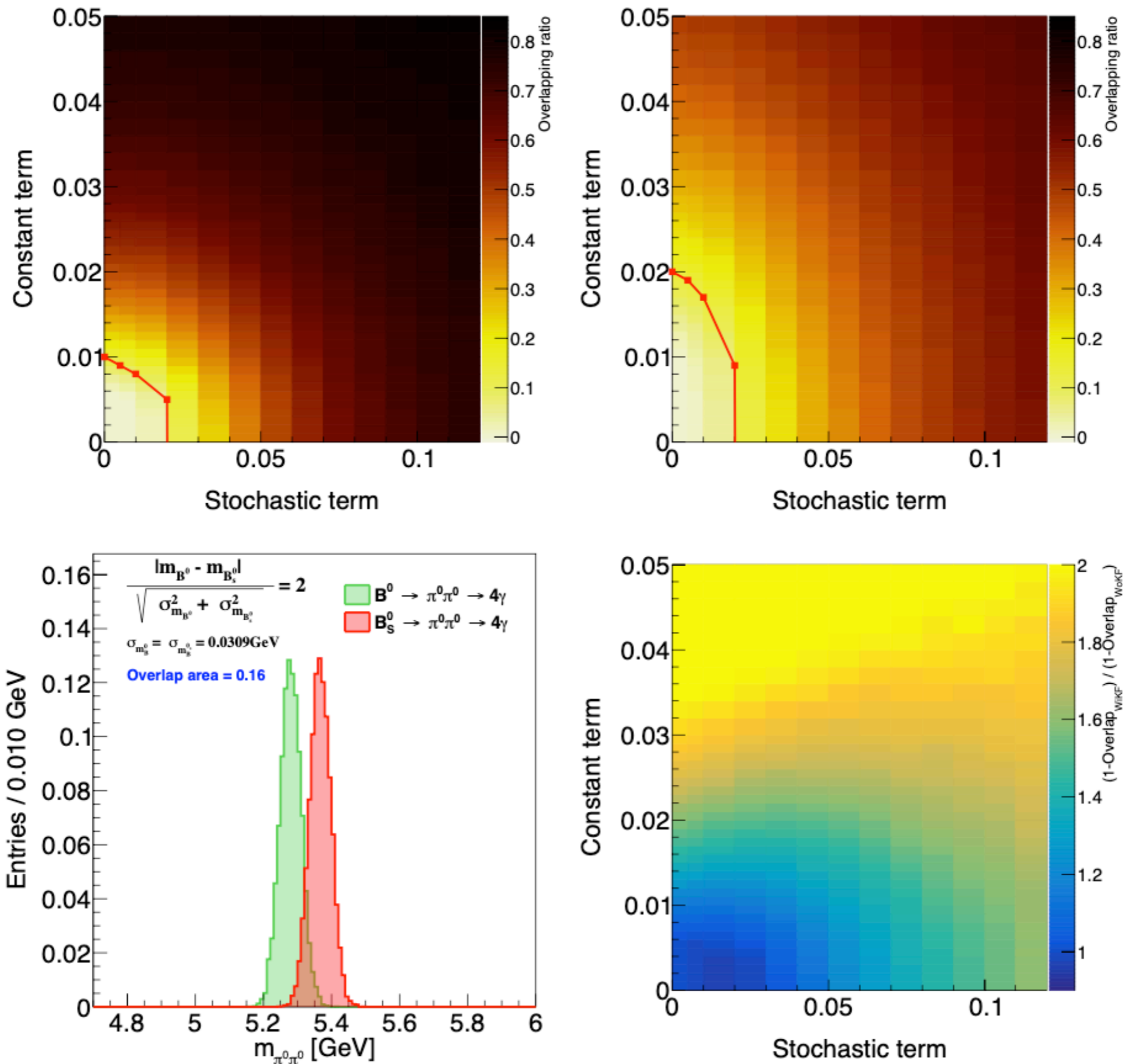


Figure 14: Separation power (overlapping area) at different ECAL resolutions wo/wi kinematic fit.